# CONSTITUTIVE MODELS FOR ENGINEERING MATERIALS

Kaspar J. Willam
University of Colorado at Boulder

## Outline

1. Introductory Remarks
2. Elastic Models
3. Elastoplastic Models
4. Analysis of Material Failure
5. Elastic Damage Models

## Glossary

**Triaxial Constitutive Models:** Algebraic, differential and integral equations relating three-dimensional stress and strain tensors.

**Elasticity:** Linear and nonlinear stress-strain relations preserving reversibility in the small (hypo-elasticity) and in the large (hyper-elasticity).

**Plasticity:** Yield constraint of stress (strain, energy) trajectory leading to irreversible deformations due to plastic flow.

**Elastic Damage Mechanics:** Degradation of elastic stiffness properties due to progressive damage.

**Failure Analysis:** Loss of stability, loss of uniqueness, and loss of ellipticity (localization) at the constitutive level.

## Opening

This article addresses constitutive models which describe the response behavior of natural and manufactured materials under different mechanical and environmental conditions. Focus of this overview is the mechanical performance of engineering materials expressed in terms of stress, strain and internal state variables which describe the effect of the previous load history on the current properties. Thereby, the domain of traditional constitutive models encompasses the continuum concepts of elasticity, plasticity, viscosity, and their extension to include thermal and other environmental effects through continuum thermodynamics.

The constitutive model introduces or describes the physical properties of a given material. It connects the kinematic with the kinetic descriptions of motion thereby closing the formulation of the initial boundary value problem. In this context it is important to keep in mind the needs of modern computational analysis techniques, such as the finite element method, which demand triaxial constitutive models for realistic model-based simulations. In fact, it is the range of the underlying material models, which delimits the predictive value of large scale simulations nowadays involving thousands of degrees of freedom. In short, our survey will concentrate on continuum-based material formulations which are currently used in engineering practice, in research and education, as well as in commercial finite element software packages

Third Edition, Volume 3, pp. 603-633,  

for stress and deformation analyses. Primary applications cover life-cycle performance assessment of civil, mechanical, and aeronautical structures ranging from dams, bridges, containment vessels, to air- and spacecraft components, as well as automotive crash simulations and micro-electro-mechanical systems.

# 1 Introductory Remarks

Traditionally, *'Material Science'* studies the behavior of materials at different scales in order to observe and quantify the chemo-physical processes at the underlying micro-mechanical, molecular and atomistic levels. Multi-scale material modeling upscales these processes onto the macroscopic level. The first step is to decompose the entire range of scales into several sub-ranges. From the view point of characterizing and designing engineering materials, we distinguish among the four scales illustrated in Figure 1:

- Meter Level:
  Practical problems in civil, mechanical and aerospace structures such as the analysis and design of dams and containment vessels are solved at this level.

- Millimeter Level:
  Most material properties are obtained from laboratory specimens at this level. In our terminology this constitutes the macro-scale - a level at which engineering materials may be treated as homogeneous continua after homogenizing the effect of the microstructural constituents into so-called *'effective'* properties.

- Micrometer Level:
  Micro-structural features such as micro-defects, the grain size of polycrystals and hydration products in cement-based materials are observed at this scale. In current terminology this constitutes the meso-scale - a level at which materials may be treated as heterogeneous composites, e.g. metal matrix and concrete composites, in which particle inclusions are bonded to the matrix by cohesive/frictional interface layers.

- Nanometer Level:
  Molecular and atomistic processes take place at this level, which includes the molecular chaining of polymers and the behavior of single crystals. Many diffusion mechanisms for moisture and aggressive chemicals are considered to be active at this level, which includes e.g. the transport process of ions and chemical compounds. It should be noted that cause-effect relations in many cases reach beyond Newtonian mechanics, especially when sub-atomic processes are considered at the level of quantum mechanics.

Historically, the current thinking of materials dates back to the *'corpuscular'* natural philosophy advanced by René Descartes (1596-1650) who postulated that the properties of matter emerge from multilevel microstructures comprised of molecules and voids. As early as 1722 René de Réaumur developed a fairly realistic picture of the anatomy and multilevel morphology of quench hardened steel in his treatise on iron at different length scales. On a separate line of materials engineering, Joseph Aspdin patented in 1824 hydraulic Portland cement for manufacturing mortar and concrete. In the historical context, the great challenge is to bridge the gap between the atomistic thinking of the classical

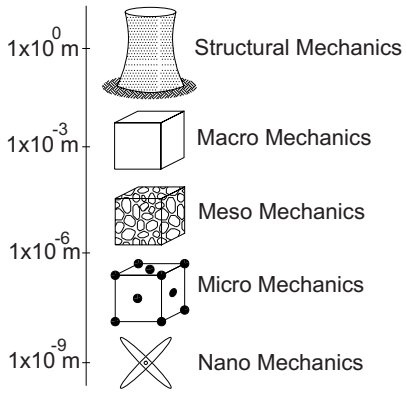


Figure 1: Multiscale Material Mechanics

greek school of natural philosophers around Democritus (460-370 b.c.), and the continuum world of differential calculus by Isaac Newton (1642-1727) and Gottfried Wilhelm Leibnitz (1646-1716), which provides the framework of modern continuum mechanics founded by Augustin Cauchy (1789-1857).

Traditionally, engineering materials are considered to be macroscopically homogeneous (and often isotropic). While in most applications this approach may be adequate, progressive degradation processes can only be explained properly by considering micro-structural features of the material. This requires characterization of each constituent and the interface bond conditions, in addition to the morphology of the specific meso- and micro-structures, respectively. These types of studies are still very demanding in terms of manpower and computing power, in spite of the rapid development of computer simulations to investigate degradation processes at the micro-, meso-, and macro- levels in 3-D space and time.

In the long history of alchemy an ancient dream is to create precious materials by synthesizing and transmuting low-cost constituents through innovative chemo-physical processes. Translated into the world of high-tech materials of today, this endeavor is at the core of *'Materials Engineering'*, where optimization and material systems engineering meet well-defined performance objectives. Consequently, the design of new high-performance materials requires thorough understanding of the properties of each constituent and their interaction in chemo-physical processes. Thereby the role of constitutive relations is to quantify the performance of the resulting material compounds under mechanical and environmental load histories. For engineering purposes the length scale under consideration is the macroscale of traditional material testing laboratories, which provide the test data to calibrate the material parameters of the constitutive relation according to specifications of the American Society for Testing and Materials, ASTM, or other professional engineering societies.

In what follows, we will review established constitutive models for engineering materials, which may be broadly classified into three groups depending on their mathematical constructs:

1. Algebraic constitutive relations, such as linear and nonlinear elastic models,
2. Differential constitutive relations, such as plastic and viscoplastic models, and
3. Integral constitutive relations, such as hereditary viscoelastic models.

Thereby it is understood that the constitutive models are linear for performance analyses under service load conditions, and highly nonlinear for limit state studies, when material failure is considered in the form of discontinuous fracture processes. For the sake of simplicity, this review will be restricted to small strains and local constitutive models in order to confine our attention to the interrelationship of stresses and strains, which are symmetric second order tensors.

The review is organized as follows: Section 2 reviews primarily isotropic elastic models and examines three families of nonlinear elastic constitutive formulations using representation theorems of scalar and tensor functions. Section 3 summarizes the flow theory of elasto-plasticity with a dicussion of volumetric-deviatoric coupling in the case of one-, two-, and three-invariant formulations. Section 4 examines material failure at the constitutive level and introduces localization analysis with an application for loading in simple shear. Section 5 briefly reviews recent developments in continuum damage mechanics. Section 6 concludes the state-of-the art report with seminal remarks on current research activities. Appendix I summarizes a few results of tensor algebra, while Appendix II contains some remarks on elastoplastic failure analysis subject to the kinematic constraint of plane strain.

## 2 Elastic Models

Linear elasticity is the main staple of material models in solids and structures. The statement *'ut tensio sic vis'* attributed to ROBERT HOOKE (1635-1703) characterizes the behavior of a linear spring in which the deformations increase proportionally with the applied forces according to the anagram *'ceiiinossstuv'*. The original format of Hooke's law included the geometric properties of the wire test specimens, and therefore the spring constant did exhibit a pronounced size effect. The definition of the modulus of elasticity $E$, where

$$\sigma = E\,\epsilon \tag{1}$$

is attributed to THOMAS YOUNG (1773-1829). He expressed the proportional material behavior through the notion of a normalized force density and a normalized deformation measure, though the original formulation also did not entirely eliminate the size effect.

The tensorial character of stress was established by Cauchy, who defined the triaxial state of stress by three traction vectors using the celebrated tetraeder argument of equilibrium. The state of stress is described in terms of Cartesian coordinates by the second order tensor

$$\boldsymbol{\sigma}(\boldsymbol{x},t) = \begin{bmatrix} \sigma_{11} & \sigma_{12} & \sigma_{13} \\ \sigma_{21} & \sigma_{22} & \sigma_{23} \\ \sigma_{31} & \sigma_{32} & \sigma_{33} \end{bmatrix} \tag{2}$$

The conjugate state of strain is a second order tensor with Cartesian coordinates,

$$\boldsymbol{\epsilon}(\boldsymbol{x},t) = \begin{bmatrix} \epsilon_{11} & \epsilon_{12} & \epsilon_{13} \\ \epsilon_{21} & \epsilon_{22} & \epsilon_{23} \\ \epsilon_{31} & \epsilon_{32} & \epsilon_{33} \end{bmatrix} \tag{3}$$

which is normally expressed in terms of the symmetric part of the displacement gradient, if we restrict our attention to infinitesimal deformations. In the case of non-polar media we may confine our attention

to stress measures, which are symmetric according to the axiom of L. Boltzmann,

$$\boldsymbol{\sigma} = \boldsymbol{\sigma}^t \quad \text{or} \quad \sigma_{ij} = \sigma_{ji} \tag{4}$$

and the conjugate strain measures

$$\boldsymbol{\epsilon} = \boldsymbol{\epsilon}^t \quad \text{or} \quad \epsilon_{ij} = \epsilon_{ji} \tag{5}$$

where $i = 1, 2, 3$ and $j = 1, 2, 3$. As a result, the eigenvalues are real-valued and constitute the set of principal stresses and strains with zero shear components in the principal eigen-directions of the second order tensor. In contrast, non-symmetric stress and strain measures may exhibit complex conjugate principal values and maximuum normal stress and strain components in directions with non-zero shear components characteristic for micropolar Cosserat continua.

Restricting this exposition to symmetric stress and strain tensors they may be cast into vector form using the Voigt notation of crystal physics.

$$\boldsymbol{\sigma}(\boldsymbol{x}, t) = \left[ \begin{array}{cccccc} \sigma_{11} & \sigma_{22} & \sigma_{33} & \tau_{12} & \tau_{23} & \tau_{31} \end{array} \right]^t \tag{6}$$

and

$$\boldsymbol{\epsilon}(\boldsymbol{x}, t) = \left[ \begin{array}{cccccc} \epsilon_{11} & \epsilon_{22} & \epsilon_{33} & \gamma_{12} & \gamma_{23} & \gamma_{31} \end{array} \right]^t \tag{7}$$

where $\tau_{ij} = \sigma_{ij}$, $\gamma_{ij} = 2\epsilon_{ij}, \forall i \neq j$. The vector form of stress and strain will allow us to formulate material models in matrix notation used predominantly in engineering, (some of the properties of second order tensors and basic tensor operations are expanded in Appendix I).

## 2.1 Linear Elastic Material Behavior:

Generalization of the scalar format of Hooke's law is based on the notion that the triaxial state of stress is proportional to the triaxial state of strain through the linear transformation,

$$\boldsymbol{\sigma} = \boldsymbol{\mathcal{E}} : \boldsymbol{\epsilon} \quad \text{or} \quad \sigma_{ij} = \mathcal{E}_{ijkl}\epsilon_{kl} \tag{8}$$

Considering the symmetry of the stress and strain, the elasticity tensor involves in general 36 elastic moduli. This may be further reduced to 21 elastic constants, if we invoke major symmetry of the elasticity tensor, i.e.

$$\boldsymbol{\mathcal{E}} = \boldsymbol{\mathcal{E}}^t \quad \text{or} \quad \mathcal{E}_{ijkl} = \mathcal{E}_{klij} \quad \text{with} \quad \mathcal{E}_{ijkl} = \mathcal{E}_{ijlk} \quad \text{and} \quad \mathcal{E}_{ijkl} = \mathcal{E}_{jikl} \tag{9}$$

The task of identifying 21 elastic moduli is simplified if we consider specific classes of symmetry, whereby orthotropic elasticity involves nine, and transversely anisotropic elasticity five elastic moduli.

1. *Isotropic Linear Elasticity*

   In the case of isotropy the fourth order elasticity tensor has the most general representation,

   $$\boldsymbol{\mathcal{E}} = a_o \mathbf{1} \otimes \mathbf{1} + a_1 \mathbf{1} \bar{\otimes} \mathbf{1} + a_2 \mathbf{1} \underline{\otimes} \mathbf{1} \quad or \quad \mathcal{E}_{ijkl} = a_o \delta_{ij}\delta_{kl} + a_1 \delta_{ik}\delta_{jl} + a_2 \delta_{il}\delta_{jk} \tag{10}$$

   where $\mathbf{1} = [\delta_{ij}]$ stands for the second order unit tensor. The three parameter expression may be recast in terms of symmetric and skew symmetric fourth order tensor components as

   $$\boldsymbol{\mathcal{E}} = a_o \mathbf{1} \otimes \mathbf{1} + b_1 \boldsymbol{\mathcal{I}} + b_2 \boldsymbol{\mathcal{I}}^{skew} \tag{11}$$

where the symmetric fourth order unit tensor reads

$$\boldsymbol{\mathcal{I}} = \frac{1}{2}[\mathbf{1}\bar{\otimes}\mathbf{1} + \mathbf{1}\underline{\otimes}\mathbf{1}] \quad or \quad \mathcal{I}_{ijkl} = \frac{1}{2}[\delta_{ik}\delta_{jl} + \delta_{il}\delta_{jk}] \tag{12}$$

and the skewed symmetric one

$$\boldsymbol{\mathcal{I}}^{skew} = \frac{1}{2}[\mathbf{1}\bar{\otimes}\mathbf{1} - \mathbf{1}\underline{\otimes}\mathbf{1}] \quad or \quad \mathcal{I}^{skew}_{ijkl} = \frac{1}{2}[\delta_{ik}\delta_{jl} - \delta_{il}\delta_{jk}] \tag{13}$$

Because of the symmetry of stress and strain the skewed symmetric contribution is inactive, $b_2 = 0$, thus isotropic linear elasticity the material behavior is fully described by two independent elastic constants. In short, the fourth order material stiffness tensor reduces to

$$\boldsymbol{\mathcal{E}} = \Lambda\mathbf{1}\otimes\mathbf{1} + 2G\boldsymbol{\mathcal{I}} \quad or \quad \mathcal{E}_{ijkl} = \Lambda\delta_{ij}\delta_{kl} + G[\delta_{ik}\delta_{jl} + \delta_{il}\delta_{jk}] \tag{14}$$

where the two elastic constants $\Lambda, G$ are named after GABRIEL LAMÉ (1795-1870).

$$\Lambda = \frac{E\ \nu}{[1+\nu][1-2\nu]} \tag{15}$$

denotes the cross modulus, and

$$G\ =\ \frac{E}{2[1+\nu]} \tag{16}$$

designates the shear modulus which have a one-to-one relationship with the modulus of elasticity and Poisson's ratio, $E, \nu$.

In the absence of initial stresses and initial strains due to environmental effects, the linear elastic relation reduces to

$$\boldsymbol{\sigma} = \Lambda[\mathrm{tr}\boldsymbol{\epsilon}]\mathbf{1} + 2G\boldsymbol{\epsilon} \quad \text{or} \quad \sigma_{ij} = \Lambda\epsilon_{kk}\delta_{ij} + 2G\epsilon_{ij} \tag{17}$$

Here the trace operation is the sum of the diagonal entries of the second order tensor corresponding to double contraction with the identity tensor $tr\boldsymbol{\epsilon} = \epsilon_{kk} = \mathbf{1} : \boldsymbol{\epsilon}$.

2. *Matrix Form of Elastic Stiffness:* $\boldsymbol{\sigma} = \boldsymbol{E}\,\boldsymbol{\epsilon}$

Isotropic linear elastic behavior may be cast in matrix format, using the Voigt notation of symmetric stress and strain tensors and the engineering definition of shear strain $\gamma_{ij} = 2\epsilon_{ij}$. The elastic stiffness matrix may be written for isotropic behavior as,

$$\boldsymbol{E} = \left[\begin{array}{ccc|ccc} \Lambda+2G & \Lambda & \Lambda & & & \\ \Lambda & \Lambda+2G & \Lambda & & 0 & \\ \Lambda & \Lambda & \Lambda+2G & & & \\ \hline & & & G & & \\ & 0 & & & G & \\ & & & & & G \end{array}\right] \tag{18}$$

3. *Matrix Form of Elastic Compliance:* $\boldsymbol{\epsilon} = \boldsymbol{C}\,\boldsymbol{\sigma}$

In the isotropic case the normal stress $\sigma_{11}$ gives rise to three normal strain contributions, the direct strain $\epsilon_{11} = \frac{1}{E}\sigma_{11}$ and the normal strains $\epsilon_{22} = -\frac{\nu}{E}\sigma_{11}, \epsilon_{33} = \frac{\nu}{E}\sigma_{11}$ because of the cross effect attributed to Siméon Denis Poisson (1781-1840). Using the principle of superposition, the additional strain contributions due to $\sigma_{22}$ and $\sigma_{33}$ enter the compliance relation for isotropic elasticity in matrix format,

$$\begin{bmatrix} \epsilon_{11} \\ \epsilon_{22} \\ \epsilon_{33} \end{bmatrix} = \frac{1}{E} \begin{bmatrix} 1 & -\nu & -\nu \\ -\nu & 1 & -\nu \\ -\nu & -\nu & 1 \end{bmatrix} \begin{bmatrix} \sigma_{11} \\ \sigma_{22} \\ \sigma_{33} \end{bmatrix} \tag{19}$$

In the isotropic case the shear response is entirely decoupled from the direct response of the normal components. Thus the compliance matrix expands into the partitioned form

$$\boldsymbol{C} = \frac{1}{E} \left[\begin{array}{ccc|ccc} 1 & -\nu & -\nu & & & \\ -\nu & 1 & -\nu & & 0 & \\ -\nu & -\nu & 1 & & & \\ \hline & & & 2[1+\nu] & & \\ & 0 & & & 2[1+\nu] & \\ & & & & & 2[1+\nu] \end{array}\right] \tag{20}$$

where isotropy entirely decouples the shear response from the normal stress-strain response. This cross effect of Poisson is illustrated in Figure 2, which shows the interaction of lateral and axial deformations under axial compression. It is intriguing that in his original work a value of $\nu = 0.25$ was proposed by S. Poisson based on molecular considerations. The elastic compliance relation

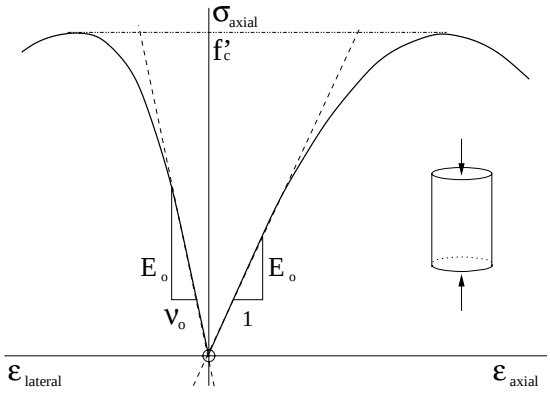


Figure 2: Poisson Effect in Axial Compression

reads in direct and indicial notations,

$$\boldsymbol{\mathcal{C}} = -\frac{\nu}{E}\mathbf{1}\otimes\mathbf{1} + \frac{1}{2G}\boldsymbol{\mathcal{I}} \quad or \quad C_{ijkl} = -\frac{\nu}{E}\delta_{ij}\delta_{kl} + \frac{1+\nu}{2E}[\delta_{ik}\delta_{jl} + \delta_{il}\delta_{jk}] \tag{21}$$

4. *Canonical Format of Isotropic Elasticity:*

Decomposing the stress and strain tensors into spherical and deviatoric components

$$\boldsymbol{s} = \boldsymbol{\sigma} - \sigma_{vol}\mathbf{1} \quad \text{where} \quad \sigma_{vol} = \frac{1}{3}[tr\boldsymbol{\sigma}] \tag{22}$$

$$\boldsymbol{e} = \boldsymbol{\epsilon} - \epsilon_{vol}\mathbf{1} \quad \text{where} \quad \epsilon_{vol} = \frac{1}{3}[tr\boldsymbol{\epsilon}] \tag{23}$$

leads to the stress deviator

$$\boldsymbol{s}(\boldsymbol{x},t) = \begin{bmatrix} \frac{1}{3}[2\sigma_{11} - \sigma_{22} - \sigma_{33}] & \sigma_{12} & \sigma_{13} \\ \sigma_{21} & \frac{1}{3}[2\sigma_{22} - \sigma_{33} - \sigma_{11}] & \sigma_{23} \\ \sigma_{31} & \sigma_{32} & \frac{1}{3}[2\sigma_{33} - \sigma_{11} - \sigma_{22}] \end{bmatrix} \tag{24}$$

and the strain deviator

$$\boldsymbol{e}(\boldsymbol{x},t) = \begin{bmatrix} \frac{1}{3}[2\epsilon_{11} - \epsilon_{22} - \epsilon_{33}] & \epsilon_{12} & \epsilon_{13} \\ \epsilon_{21} & \frac{1}{3}[2\epsilon_{22} - \epsilon_{33} - \epsilon_{11}] & \epsilon_{23} \\ \epsilon_{31} & \epsilon_{32} & \frac{1}{3}[2\epsilon_{33} - \epsilon_{11} - \epsilon_{22}] \end{bmatrix} \tag{25}$$

which have the property $tr\boldsymbol{s} = 0$ and $tr\boldsymbol{e} = 0$. The decomposition decouples the volumetric from the distortional response, because of the underlying orthogonality of the spherical and deviatoric partitions, $\boldsymbol{s} : [\sigma_{vol}\mathbf{1}] = 0$ and $\boldsymbol{e} : [\epsilon_{vol}\mathbf{1}] = 0$. The decoupled response reduces the elasticity tensor to the scalar form,

$$\sigma_{vol} = 3\,K\epsilon_{vol} \quad \text{and} \quad \boldsymbol{s} = 2\,G\boldsymbol{e} \tag{26}$$

in which the bulk and the shear moduli,

$$K = \frac{E}{3[1-2\nu]} = \Lambda + \frac{2}{3}G \quad \text{and} \quad G = \frac{E}{2[1+\nu]} = \frac{3}{2}[K - \Lambda] \tag{27}$$

define the volumetric and the deviatoric material stiffness.

Consequently, the internal strain energy density expands into the canonical form of two decoupled contributions

$$2W = \boldsymbol{\sigma} : \boldsymbol{\epsilon} = [\sigma_{vol}\mathbf{1}] : [\epsilon_{vol}\mathbf{1}] + \boldsymbol{s} : \boldsymbol{e} = 9\,K\epsilon_{vol}^2 + 2G\boldsymbol{e} : \boldsymbol{e} \tag{28}$$

such that the positive strain energy argument delimits the range of possible values of Poisson's ratio to $-1 \leq \nu \leq 0.5$

### 2.1.1 Isotropic Elasticity under Initial Volumetric Strain

In the case of isotropic material behavior, with no directional properties, the size of a representative volume element may change due to thermal effects or shrinkage and swelling, but it will not distort. Consequently, the expansion is purely volumetric, i.e. identical in all directions. Using direct and indicial

notation, the additive decomposition of strain into elastic and initial volumetric components, $\boldsymbol{\epsilon} = \boldsymbol{\epsilon}_e + \boldsymbol{\epsilon}_o$, leads to the following extension of the elastic compliance relation:

$$\boldsymbol{\epsilon} = -\frac{\nu}{E}[tr\boldsymbol{\sigma}]\mathbf{1} + \frac{1}{2G}\boldsymbol{\sigma} + \epsilon_o\mathbf{1} \quad \text{or} \quad \epsilon_{ij} = -\frac{\nu}{E}\sigma_{kk}\delta_{ij} + \frac{1}{2G}\sigma_{ij} + \epsilon_o\delta_{ij} \tag{29}$$

where $\boldsymbol{\epsilon}_o = \epsilon_o\mathbf{1}$ denotes the initial volumetric strain e.g. due to thermal expansion. The inverse relation reads

$$\boldsymbol{\sigma} = \Lambda[tr\boldsymbol{\epsilon}]\mathbf{1} + 2G\boldsymbol{\epsilon} - 3\epsilon_o K\mathbf{1} \quad \text{or} \quad \sigma_{ij} = \Lambda\epsilon_{kk}\delta_{ij} + 2G\epsilon_{ij} - 3\epsilon_o K\delta_{ij} \tag{30}$$

Rewriting this equation in matrix notation we have:

$$\begin{bmatrix}\sigma_{11}\\ \sigma_{22}\\ \sigma_{33}\end{bmatrix} = \begin{bmatrix}K+\frac{4}{3}G & K-\frac{2}{3}G & K-\frac{2}{3}G\\ K-\frac{2}{3}G & K+\frac{4}{3}G & K-\frac{2}{3}G\\ K-\frac{2}{3}G & K-\frac{2}{3}G & K+\frac{4}{3}G\end{bmatrix}\begin{bmatrix}\epsilon_{11}\\ \epsilon_{22}\\ \epsilon_{33}\end{bmatrix} - 3K\epsilon_o\begin{bmatrix}1\\1\\1\end{bmatrix} \tag{31}$$

Considering the special case of plane stress, $\sigma_{33} = 0$, the stress-strain relations reduce in the presence of initial volumetric strains to:

$$\begin{bmatrix}\sigma_{11}\\ \sigma_{22}\end{bmatrix} = \frac{E}{1-\nu^2}\begin{bmatrix}1 & \nu\\ \nu & 1\end{bmatrix}\begin{bmatrix}\epsilon_{11}\\ \epsilon_{22}\end{bmatrix} - \frac{E}{1-\nu}\epsilon_o\begin{bmatrix}1\\1\end{bmatrix} \tag{32}$$

where the shear components are not affected by the temperature change in the case of isotropy.

### 2.1.2 Free Thermal Expansion

Under stress free conditions the thermal expansion $\boldsymbol{\epsilon}_o = \alpha[T - T_o]\mathbf{1}$ leads to $\boldsymbol{\epsilon} = \boldsymbol{\epsilon}_o$, i.e.

$$\epsilon_{11} = \alpha[T - T_o] \tag{33}$$
$$\epsilon_{22} = \alpha[T - T_o] \tag{34}$$
$$\epsilon_{33} = \alpha[T - T_o] \tag{35}$$

Thus the change of temperature results in free thermal expansion, while the mechanical stress remains zero under zero confinement, $\boldsymbol{\sigma} = \boldsymbol{\mathcal{E}} : \boldsymbol{\epsilon}_e = \mathbf{0}$.

### 2.1.3 Thermal Stress under Full Confinement

In contrast to the unconfined situation above, the thermal expansion is equal and opposite to the elastic strain $\boldsymbol{\epsilon}_e = -\boldsymbol{\epsilon}_o$ under full confinement, when $\boldsymbol{\epsilon} = 0$. In the case of plane stress, the temperature change $\Delta T = T - T_o$ leads to the thermal stresses

$$\sigma_{11} = -\frac{E}{1-\nu}\alpha[T - T_o] \tag{36}$$
$$\sigma_{22} = -\frac{E}{1-\nu}\alpha[T - T_o] \tag{37}$$

## 2.2 Nonlinear Elasticity

In linear elasticity the resulting constitutive relations do not depend on the point of departure, except for the symmetry argument, which is derived most naturally from the energy argument. In contrast, nonlinear elastic material models strongly depend on the setting of the constitutive formulation. Considering for a moment the uniaxial stress-strain relation shown in Figure 3, it appears that the nonlinear material law may be formulated in terms of any one of the following three possibilities:

(a) Algebraic Format: $\boldsymbol{\sigma} = \boldsymbol{f}(\boldsymbol{\epsilon})$

The algebraic format extends Hooke's law $\boldsymbol{\sigma} = \boldsymbol{\mathcal{E}} : \boldsymbol{\epsilon}$ into the nonlinear regime. The triaxial generalization of the scalar-valued algebraic function leads in the simplest case to the concept of a secant stiffness, $\boldsymbol{\sigma} = \boldsymbol{E}_s : \boldsymbol{\epsilon}$. In the triaxial situation this leads to the question how to represent a symmetric tensor-valued function of the symmetric strain tensor, $\boldsymbol{\sigma} = \boldsymbol{f}(\boldsymbol{\epsilon})$. This type of constitutive model is limited to rate and history independent material behavior, such as linear and nonlinear elasticity which do not exhibit hysteretic effects.

(b) Integral Format: $\boldsymbol{\sigma} = \frac{\partial W}{\partial \boldsymbol{\epsilon}}$

The integral format is the repository of functional representations which include linear and nonlinear viscoelasticity in which creep and relaxation are considered in the form of fading memory effects, $\boldsymbol{\sigma}(t) = \boldsymbol{\mathcal{F}}_{t_o \le \tau \le t} \frac{\partial W(\boldsymbol{\epsilon}(\tau), \boldsymbol{q})}{\partial \boldsymbol{\epsilon}}$. As long as the rate sensitivity does not include any history effects, $\boldsymbol{q} = \boldsymbol{0}$, the functional representation does not exhibit hysteretic effects. In this case and in the absence of rate dependence we recover the format of instantaneous hyperelasticity, in which the stress is derived from the gradient of an elastic potential, $\boldsymbol{\sigma} = \frac{\partial W}{\partial \boldsymbol{\epsilon}}$.

(c) Differential Format: $d\boldsymbol{\sigma} = \boldsymbol{E}_t : d\boldsymbol{\epsilon}$

In its elementary format the differential form reduces to the tangential stress-strain relationship. In a broader sense it provides also a repository for internal variables, which memorize inelastic changes of the material properties in plasticity and viscoplasticity. In this case, hysteretic effects are included to account for material dissipation and energy release in the case of fracture. Restricting our attention to nonlinear hypolasticity, the differential format leads to the question how to represent the stress rate in terms of a tensor-valued function of two symmetric tensors, $\dot{\boldsymbol{\sigma}} = \boldsymbol{g}(\boldsymbol{\sigma}, \dot{\boldsymbol{\epsilon}})$?

In what follows we will see that the three versions of nonlinear elasticity lead to constitutive formulations which exhibit fundamental differences when we consider triaxial conditions.

### 2.2.1 Algebraic Format

The so-called 'total' stress–strain relation expresses stress in terms of a nonlinear function of strain. As an alternative, the secant relation, $\boldsymbol{\sigma} = \boldsymbol{\mathcal{E}}_s : \boldsymbol{\epsilon}$ provides a pseudo-linear format, which simply redefines the nonlinear function $\boldsymbol{f}(\boldsymbol{\epsilon})$ in terms of the nonlinear secant modulus $\boldsymbol{\mathcal{E}}_s$.

The triaxial setting, however, leads to two algebraic formats of nonlinear elasticity which differ in a fundamental manner:

1. *Cauchy Elasticity:* $\boldsymbol{\sigma} = \boldsymbol{f}(\boldsymbol{\epsilon})$

   In this case, the triaxial state of stress is a nonlinear tensor function of the strain tensor, i.e. in indicial notation $\sigma_{ij} = f_{ij}(\epsilon_{kl})$. Using the representation theorems of second order symmetric

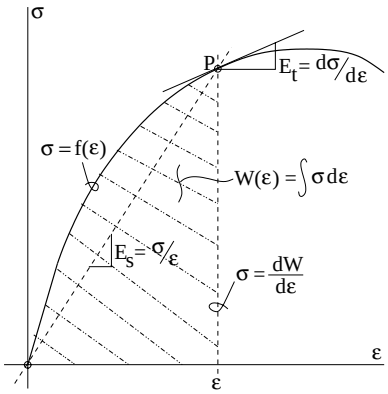


Figure 3: Conceptual Material Models of Nonlinear Elasticity

tensor functions the possibilities are restricted to a small set of possible choices when isotropy is invoked. In this case, the most general format of Cauchy elasticity may have one of the two representations,

$$\boldsymbol{\sigma} = \Phi_1 \mathbf{1} + \Phi_2 \boldsymbol{\epsilon} + \Phi_3 \boldsymbol{\epsilon}^2 \quad \text{or} \quad \boldsymbol{\sigma} = \Psi_1 \mathbf{1} + \Psi_2 \boldsymbol{\epsilon} + \Psi_3 \boldsymbol{\epsilon}^{-1} \tag{38}$$

because of the Cayleigh-Hamilton theorem. Thereby, the three response functions $\Phi_i$, and $\Psi_i$ are scalar functions of the three invariants of either stress or strain. It is important to keep in mind that Cauchy elasticity is based on a second order symmetric tensor function of a second order symmetric tensor.

2. *Secant or Pseudo-Elasticity:* $\boldsymbol{\sigma} = \boldsymbol{\mathcal{E}}_s : \boldsymbol{\epsilon}$

   In the pseudo-elastic format of elasticity, the nonlinearity is incorporated into the fourth order secant stiffness tensor. This format has been used early on in different engineering disciplines to develop nonlinear extensions of simple classes of linear elasticity. The so-called variable stiffness models retain the format of linear elasticity and simply replace the two elastic constants of linear elasticity by nonlinear functions. We will see later on that the nonlinear $K-G$ models are theoretically sound if the nonlinear response decouples the volumetric from the deviatoric response, i.e. $K = K(\epsilon_{vol})$ and $G = G(tr\boldsymbol{e}^2)$ where $tr\boldsymbol{e}^2 = \boldsymbol{e} : \boldsymbol{e}$.

   It is not very surprising that elastic damage models did start from this secant format of nonlinear elasticity using arguments of effective stiffness properties, which are in some sense equivalent to distributed micro-mechanical defects. In fact, the original proposal of scalar damage was nothing but a nonlinear pseudo-elastic model in which the secant stiffness is in matrix notation

$$\boldsymbol{\sigma} = \boldsymbol{E}_s \boldsymbol{\epsilon} \quad \text{where} \quad \boldsymbol{E}_s = [1-d]\boldsymbol{E}_o \quad \text{and} \quad d = 1 - \frac{E_s}{E_o} \tag{39}$$

   In its basic format the secant matrix of elastic damage retains the structure of the initial elastic

stiffness except for the factor $[1-d]$

$$\boldsymbol{E}_s = \frac{[1-d]E_o}{[1+\nu_o][1-2\nu_o]} \left[\begin{array}{ccc|ccc} 1-\nu_o & \nu_o & \nu_o & & & \\ \nu_o & 1-\nu_o & \nu_o & & 0 & \\ \nu_o & \nu_o & 1-\nu_o & & & \\ \hline & & & \frac{1-2\nu_o}{2} & & \\ & 0 & & & \frac{1-2\nu_o}{2} & \\ & & & & & \frac{1-2\nu_o}{2} \end{array}\right] \tag{40}$$

which measures the remaining integrity of the material when the damage variable increases from zero to one, $0 \leq d \to 1$. Restricting damage to the format of isotropic linear elasticity, it is natural to decompose degradation into volumetric and deviatoric damage components such that

$$K_s = [1-d_{vol}]K_o \quad \text{and} \quad G_s = [1-d_{dev}]G_o \tag{41}$$

The corresponding secant relation of elastic damage reads in matrix notation

$$\boldsymbol{E}_s = \left[\begin{array}{ccc|ccc} K_s+\frac{4}{3}G_s & K_s-\frac{2}{3}G_s & K_s-\frac{2}{3}G_s & & & \\ K_s-\frac{2}{3}G_s & K_s+\frac{4}{3}G_s & K_s-\frac{2}{3}G_s & & 0 & \\ K_s-\frac{2}{3}G_s & K_s-\frac{2}{3}G_s & K_s+\frac{4}{3}G_s & & & \\ \hline & & & G_s & & \\ & 0 & & & G_s & \\ & & & & & G_s \end{array}\right] \tag{42}$$

From this expression we observe that the secant format of isotropic elastic damage is very simple because of the underlying decoupling of volumetric from deviatoric degradation. As long as we are only interested in a given state of damage, this isotropic pseudo-elastic formulation suffices to describe the response behavior using effective material properties based on the principle of stress- or strain equivalence. However, the constitutive formulation becomes far more intricate when a thermodynamically consistent damage formulation is needed for progressive damage simulations. In this case, loading and unloading have to be defined for the general case of triaxial conditions, and evolution laws are required to describe the two independent processes of volumetric and deviatoric damage which will be described in Section 5 in more detail.

### 2.2.2 Integral Format

The integral description of elasticity starts from the postulate of a strain energy function from which the stress is derived by differentiation. This 'hyperelastic' format of elasticity dates back to the original work of George Green (1793-1841).

1. *Green Elasticity:* $\boldsymbol{\sigma} = \frac{\partial W}{\partial \boldsymbol{\epsilon}}$

Given a strain energy density potential, $W = W(\boldsymbol{\epsilon})$, the hyperelastic stress-strain relation is simply the gradient of that potential function with respect to strain,

$$\boldsymbol{\sigma} = \frac{\partial W}{\partial \boldsymbol{\epsilon}} \quad \text{or} \quad \sigma_{ij} = \frac{\partial W}{\partial \epsilon_{ij}} \tag{43}$$

The compliance relation derives from the dual complementary strain energy potential. The important aspect of this integral formulation is the path-independence of the line integral which defines the internal strain energy

$$W(\boldsymbol{\epsilon}) = \int_{\epsilon} \boldsymbol{\sigma} : d\boldsymbol{\epsilon} = \int_{\epsilon} \frac{\partial W}{\partial \boldsymbol{\epsilon}} : d\boldsymbol{\epsilon} = \int_{\epsilon} dW \tag{44}$$

in terms of the total differential $dW$. The traditional notions of elasticity, such as reversibility and lack of energy dissipation under closed cycles of strain, are a direct consequence of path-independence, i.e.

$$W(\boldsymbol{\epsilon}) = \oint_{\epsilon} dW = 0 \tag{45}$$

In other terms, the hyperelastic material description is non-dissipative and preserves energy under arbitrary strain histories.

The corresponding hyperelastic stiffness tensor is a measure of the curvature of the strain energy function involving the second derivatives of $W = W(\boldsymbol{\epsilon})$,

$$\dot{\boldsymbol{\sigma}} = \boldsymbol{\mathcal{E}}_t : \dot{\boldsymbol{\epsilon}} \quad \text{where} \quad \boldsymbol{\mathcal{E}}_t = \frac{\partial^2 W}{\partial \boldsymbol{\epsilon} \otimes \partial \boldsymbol{\epsilon}} \tag{46}$$

Consequently, the elasticity tensor is symmetric, $\boldsymbol{\mathcal{E}}_t = \boldsymbol{\mathcal{E}}_t^t$, if $W(\boldsymbol{\epsilon})$ is sufficiently smooth. This reduces the 36 elastic constants to 21 in the general case of anisotropic elasticity, and to two in case of isotropy. The positive definiteness of the hyperelastic tangent operator, $\det \boldsymbol{\mathcal{E}}_t > 0$, is directly connected to the convexity of the strain energy functional and the uniqueness argument of boundary value problems in elasticity.

2. *Isotropic Hyperelastic Models:*

In the case of isotropy, frame-objectivity requires that the strain energy density function must be independent from the coordinate system of an observer. Thus the potential function must be a function of strain invariants and combinations thereof. In the past two different families of nonlinear isotropic hyperelastic material models have been proposed, one leads to the format of nonlinear K-G models, while the other results in a pseudo-orthotropic format based on principal coordinates of stress and strain.

(a) Hyperelastic K-G Models:
Starting from the invariant representation of the strain energy density function, $W(\boldsymbol{\epsilon}) = W(I_1, I_2, I_3)$, the stress-strain relation follows from the chain rule of differentiation as:

$$\boldsymbol{\sigma} = \frac{\partial W}{\partial \boldsymbol{\epsilon}} = \frac{\partial W}{\partial I_1}\frac{\partial I_1}{\partial \boldsymbol{\epsilon}} + \frac{\partial W}{\partial I_2}\frac{\partial I_2}{\partial \boldsymbol{\epsilon}} + \frac{\partial W}{\partial I_3}\frac{\partial I_3}{\partial \boldsymbol{\epsilon}} \tag{47}$$

Using the moment invariants for the sake of convenience, where $I_i = \frac{1}{i} tr\boldsymbol{\epsilon}^i$, the derivatives simplify to $\frac{\partial I_i}{\partial \boldsymbol{\epsilon}} = \boldsymbol{\epsilon}^{i-1}$. Consequently, the nonlinear isotropic stress-strain relation results in the general hyperelastic format for nonlinear isotropic behavior,

$$\boldsymbol{\sigma} = W_1 \mathbf{1} + W_2 \boldsymbol{\epsilon} + W_3 \boldsymbol{\epsilon}^2 \tag{48}$$

The three scalar functions $W_i = \frac{\partial W}{\partial I_i} = W_i(I_j)$ describe the degree of nonlinearity in terms of three irreducible invariants, while the tensorial properties are characterized by the three irreducible basis tensors $\mathbf{1}, \boldsymbol{\epsilon}, \boldsymbol{\epsilon}^2$. Note the interrelationship between the scalar functions,

$$\frac{\partial W_i}{\partial I_j} = \frac{\partial W_j}{\partial I_i} \quad \text{since} \quad \frac{\partial^2 W}{\partial I_i \partial I_j} = \frac{\partial^2 W}{\partial I_j \partial I_i} \tag{49}$$

when they are derived from a sufficiently differentiable scalar potential, $W = W(I_1, I_2, I_3)$. In contrast, the scalar functions $\Phi_i$ and $\Psi_i$ of the pseudo-elastic formulation do not satisfy this form of reciprocity if the underlying integrability conditions are not enforced.

On the issue of volumetric-deviatoric coupling we observe that the trace operation leads to

$$tr\boldsymbol{\sigma} = 3W_1 + W_2 tr\boldsymbol{\epsilon} + W_3 tr\boldsymbol{\epsilon}^2 \tag{50}$$

Considering a simple shear deformation, with $\epsilon_{12} = 0.5\gamma$, $W_3$ and thus the dependence of $W = W(I_1, I_2, I_3)$ on the third invariant is responsible for volumetric-deviatoric interaction.

On another note, the quadratic expansion of the strain energy density function with leads exactly to the two Lamé constants of linear isotropic elasticity since $W_3 = 0$. Thus it is Green hyperelasticity which firmly established the bi-modular theory of isotropic elasticity in contrast to the uni-modular theory which was widely accepted by the French school of engineering scientists in the last century.

In fact, this bi-modular format also holds for nonlinear hyperelasticity if the strain energy density function can be decomposed into two independent functions, one defining the volumetric and the other the deviatoric behavior.

$$W(\boldsymbol{\epsilon}) = W_{vol}(tr\boldsymbol{\epsilon}) + W_{dev}(tr\boldsymbol{e}^2) \tag{51}$$

This infers, however, that the influence of the third invariant $I_3$ remains negligible, since it is this term which is responsible for coupling the volumetric and deviatoric response behavior. The decomposition of the strain energy function leads to the appealing concept of nonlinear $K - G$ models, because of their inherent simplicity, which retains the two-modular form of linear elasticity. Figures 4 and 5 illustrate the secant stiffness relations, which may be expressed best in the form of the octahedral components of stress $\sigma_o, \tau_o$ and strain $\epsilon_o, \gamma_o$,

$$\begin{bmatrix} \sigma_o \\ \tau_o \end{bmatrix} = \begin{bmatrix} 3K_s & 0 \\ 0 & 2G_s \end{bmatrix} \begin{bmatrix} \epsilon_o \\ \gamma_o \end{bmatrix} \tag{52}$$

where $K_s = K(tr\boldsymbol{\epsilon})$ and $G_s = G(tr\boldsymbol{e}^2)$. The so-called $K - G$ models shown in Figures 4 and 5 play a prominent role for modeling nonlinear material behavior.

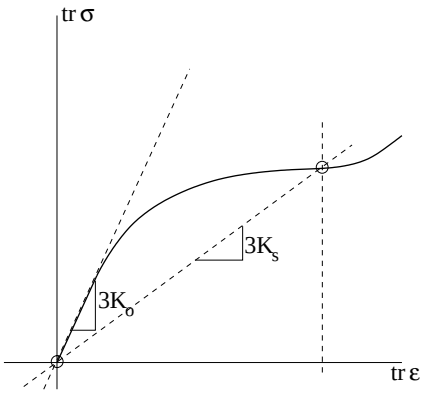


Figure 4: Nonlinear Volumetric Response Behavior

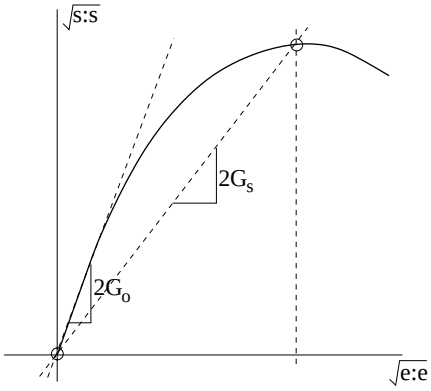


Figure 5: Nonlinear Deviatoric Response Behavior

Combining the volumetric and deviatoric scalar relations leads to the secant stiffness relation

$$\boldsymbol{\sigma} = \boldsymbol{\mathcal{E}}_s : \boldsymbol{\epsilon} \quad \text{where} \quad \boldsymbol{\mathcal{E}}_s = [K_s - \frac{2}{3}G_s]\mathbf{1} \otimes \mathbf{1} + 2G_s\boldsymbol{\mathcal{I}} \tag{53}$$

where the elastic material constants have been simply replaced by their secant values. The corresponding tangential stiffness relation however introduces an additional fourth order tensor term because of the chain rule of differentiation when taking derivatives of $G_s = G_s(\sqrt{\boldsymbol{e} : \boldsymbol{e}})$,

$$\dot{\boldsymbol{\sigma}} = \boldsymbol{\mathcal{E}}_t : \dot{\boldsymbol{\epsilon}} \quad \text{where} \quad \boldsymbol{\mathcal{E}}_t = [K_t - \frac{2}{3}G_s]\mathbf{1} \otimes \mathbf{1} + 2G_s\boldsymbol{\mathcal{I}} + \frac{4[G_t - G_s]}{tr\boldsymbol{e}^2}\boldsymbol{e} \otimes \boldsymbol{e} \tag{54}$$

The dyadic tensor product $\boldsymbol{e} \otimes \boldsymbol{e}$ originates from the nonlinearity and reflects the state of the deviator strain on the incremental material law. This term is the source of strain-induced anisotropy, which characterizes the tangential stiffness relations of all elastoplastic and elastic damage models.

(b) Hyperelastic Model in Principal Coordinates:
In this case the strain energy function is expressed in terms of the principal strain values,

$$W = W(\epsilon_1, \epsilon_2, \epsilon_3) = W(\epsilon_2, \epsilon_3, \epsilon_1) = W(\epsilon_3, \epsilon_1, \epsilon_2) \tag{55}$$

whereby the underlying isotropy infers cyclic permutation of indices. Because of the underlying coaxiality of the principal axes of stress and strain, the stress-strain relation involves only their principal values, i.e.

$$\sigma_i = \frac{\partial W(\epsilon_1, \epsilon_2, \epsilon_3)}{\partial \epsilon_i} \tag{56}$$

The tangential stress-strain relation leads to the following matrix representation of the principal coordinates:

$$\begin{bmatrix} \dot{\sigma}_1 \\ \dot{\sigma}_2 \\ \dot{\sigma}_3 \end{bmatrix} = \begin{bmatrix} \frac{\partial^2 W}{\partial \epsilon_1 \partial \epsilon_1} & \frac{\partial^2 W}{\partial \epsilon_1 \partial \epsilon_2} & \frac{\partial^2 W}{\partial \epsilon_1 \partial \epsilon_3} \\ \frac{\partial^2 W}{\partial \epsilon_2 \partial \epsilon_1} & \frac{\partial^2 W}{\partial \epsilon_2 \partial \epsilon_2} & \frac{\partial^2 W}{\partial \epsilon_2 \partial \epsilon_3} \\ \frac{\partial^2 W}{\partial \epsilon_3 \partial \epsilon_1} & \frac{\partial^2 W}{\partial \epsilon_3 \partial \epsilon_2} & \frac{\partial^2 W}{\partial \epsilon_3 \partial \epsilon_3} \end{bmatrix} \begin{bmatrix} \dot{\epsilon}_1 \\ \dot{\epsilon}_2 \\ \dot{\epsilon}_3 \end{bmatrix} \tag{57}$$

This illustrates the symmetry of the tangential stiffness properties if the strain energy function is sufficiently smooth. Moreover, the tangential stiffness properties are positive definite if the strain energy function remains convex. Although the tangential relation appears to be anisotropic in principal coordinates, the nonlinear stress-strain rate relation maintains coaxiality between $\boldsymbol{\sigma} - \boldsymbol{\epsilon}$ as long as the tangential shear terms satisfy the condition, R. Ogden [1984]:

$$\begin{bmatrix} \dot{\tau}_{12} \\ \dot{\tau}_{23} \\ \dot{\tau}_{31} \end{bmatrix} = \begin{bmatrix} \frac{\sigma_2 - \sigma_1}{\epsilon_2 - \epsilon_1} & 0 & 0 \\ 0 & \frac{\sigma_3 - \sigma_2}{\epsilon_3 - \epsilon_2} & 0 \\ 0 & 0 & \frac{\sigma_1 - \sigma_3}{\epsilon_1 - \epsilon_3} \end{bmatrix} \begin{bmatrix} \dot{\gamma}_{12} \\ \dot{\gamma}_{23} \\ \dot{\gamma}_{31} \end{bmatrix} \tag{58}$$

In the past, the principal coordinate representation of nonlinear stress-strain relations has been popularized under the name of 'orthotropic' material models, see Chen & Han [1988], though strictly speaking the constitutive format is isotropic in which the strain-induced orthotropy appears because of the different levels of nonlinearity in the principal coordinates.

### 2.2.3 Differential Format

The differential description of elasticity starts from representation theorems of nonlinear tensor functions which lead in the simplest case of grade-one materials to an incrementally linear format of tangential stiffness. The 'hypoelastic' terminology is attributed to Clifford Truesdell (1919-2000), although the linear format of incremental elasticity is normally referred to as tangential stiffness model.

1. *Truesdell Elasticity*: $\dot{\boldsymbol{\sigma}} = \boldsymbol{g}(\boldsymbol{\sigma}, \dot{\boldsymbol{\epsilon}})$

   In the differential format of elasticity the stress rate is expanded into a symmetric tensor function of two second order tensors. In the case of a stress-based formulation, the two independent arguments of the tensor function are the stress and the rate of strain tensors. Invoking the argument of material objectivity and frame indifference, the irreducible set of base tensors encompasses the following terms:

$$\mathbf{1}, \boldsymbol{\sigma}, \boldsymbol{\sigma}^2, \dot{\boldsymbol{\epsilon}}, \dot{\boldsymbol{\epsilon}}^2, (\boldsymbol{\sigma} \cdot \dot{\boldsymbol{\epsilon}} + \dot{\boldsymbol{\epsilon}} \cdot \boldsymbol{\sigma}), (\boldsymbol{\sigma} \cdot \dot{\boldsymbol{\epsilon}}^2 + \dot{\boldsymbol{\epsilon}}^2 \cdot \boldsymbol{\sigma}), (\boldsymbol{\sigma}^2 \cdot \dot{\boldsymbol{\epsilon}} + \dot{\boldsymbol{\epsilon}} \cdot \boldsymbol{\sigma}^2), (\boldsymbol{\sigma}^2 \cdot \dot{\boldsymbol{\epsilon}}^2 + \dot{\boldsymbol{\epsilon}}^2 \cdot \boldsymbol{\sigma}^2) \tag{59}$$

Conseqently, an isotropic tensor function of two symmetric tensors involves in the most general case nine response functions, $\phi_1, ..\phi_9$ which depend in turn on the six moment invariants of the stress and strain rate tensors below,

$$\bar{I}_1^{\sigma} = tr\boldsymbol{\sigma},\ \bar{I}_2^{\sigma} = tr\boldsymbol{\sigma}^2,\ \bar{I}_3^{\sigma} = tr\boldsymbol{\sigma}^3;\ \bar{I}_1^{\dot{\epsilon}} = tr\dot{\boldsymbol{\epsilon}},\ \bar{I}_2^{\dot{\epsilon}} = tr\dot{\boldsymbol{\epsilon}}^2,\ \bar{I}_3^{\dot{\epsilon}} = tr\dot{\boldsymbol{\epsilon}}^3 \tag{60}$$

as well as on the four joint invariants

$$\bar{J}_1 = tr(\boldsymbol{\sigma} \cdot \dot{\boldsymbol{\epsilon}}),\ \bar{J}_2 = tr(\boldsymbol{\sigma}^2 \cdot \dot{\boldsymbol{\epsilon}}),\ \bar{J}_3 = tr(\boldsymbol{\sigma} \cdot \dot{\boldsymbol{\epsilon}}^2),\ \bar{J}_4 = tr(\boldsymbol{\sigma}^2 \cdot \dot{\boldsymbol{\epsilon}}^2) \tag{61}$$

The general format results in the general stress-strain rate relation,

$$\dot{\boldsymbol{\sigma}} = \phi_1\mathbf{1}+\phi_2\boldsymbol{\sigma}+\phi_3\boldsymbol{\sigma}^2+\phi_4\dot{\boldsymbol{\epsilon}}+\phi_5\dot{\boldsymbol{\epsilon}}^2+\phi_6(\boldsymbol{\sigma}\cdot\dot{\boldsymbol{\epsilon}}+\dot{\boldsymbol{\epsilon}}\cdot\boldsymbol{\sigma})+\phi_7(\boldsymbol{\sigma}\cdot\dot{\boldsymbol{\epsilon}}^2+\dot{\boldsymbol{\epsilon}}^2\cdot\boldsymbol{\sigma})+\phi_8(\boldsymbol{\sigma}^2\cdot\dot{\boldsymbol{\epsilon}}+\dot{\boldsymbol{\epsilon}}\cdot\boldsymbol{\sigma}^2)+\phi_9(\boldsymbol{\sigma}^2\cdot\dot{\boldsymbol{\epsilon}}^2+\dot{\boldsymbol{\epsilon}}^2\cdot\boldsymbol{\sigma}^2) \tag{62}$$

For rate independence, the expansion must be homogeneous of order one, thus the rate terms of the tensor function must be restricted to the first order. In other terms, the hypo-elastic material law is rate independent, if and only if,

$$\boldsymbol{g}(\boldsymbol{\sigma}, \alpha\dot{\boldsymbol{\epsilon}}) = \alpha\boldsymbol{g}(\boldsymbol{\sigma}, \dot{\boldsymbol{\epsilon}}) \tag{63}$$

Among the numerous possibilities, two classes of hypoelastic constitutive models may be distinguished.

(a) Incrementally Linear Hypoelastic Models:
The linear restriction of the hypoelastic stress-strain relations leads to the classical tangential stiffness format

$$\dot{\boldsymbol{\sigma}} = \boldsymbol{\mathcal{E}}_t : \dot{\boldsymbol{\epsilon}} \quad \text{where} \quad \boldsymbol{\mathcal{E}}_t = \boldsymbol{\mathcal{E}}(\boldsymbol{\sigma}) \tag{64}$$

This stress-based format is reversible in the small, but not in the large. In other terms, the classical hypoelastic formulation leads to path-dependence

$$\boldsymbol{\sigma} = \int_{\epsilon} \boldsymbol{\mathcal{E}}_t(\boldsymbol{\sigma}) : \frac{d\boldsymbol{\epsilon}}{dt} dt \tag{65}$$

This infers energy dissipation and irreversible behavior for arbitrary load histories as opposed to hyperelasticity. In fact, the hyperelastic property of path-independence is recovered only if appropriate integrability conditions are satisfied which assure that the stress is the gradient of a single potential function, i.e. $\boldsymbol{\sigma} = \frac{\partial W}{\partial \boldsymbol{\epsilon}}$.

The most general format of the hypoelastic tangent operator involves 12 hypoelastic response functions which depend in general on all ten stress invariants, $C_i = C_i(I_j, J_k)$. The tensorial structure involves twelve fourth order tensor products between the second order unit tensor and stress tensors up to the fourth power.

$$\boldsymbol{\mathcal{E}}_t = \begin{bmatrix} C_1\mathbf{1}\otimes\mathbf{1} & +C_2\boldsymbol{\sigma}\otimes\mathbf{1} & +C_3\boldsymbol{\sigma}^2\otimes\mathbf{1} \\ +C_4\mathbf{1}\otimes\boldsymbol{\sigma} & +C_5\boldsymbol{\sigma}\otimes\boldsymbol{\sigma} & +C_6\boldsymbol{\sigma}^2\otimes\boldsymbol{\sigma} \\ +C_7\mathbf{1}\otimes\boldsymbol{\sigma}^2 & +C_8\boldsymbol{\sigma}\otimes\boldsymbol{\sigma}^2 & +C_9\boldsymbol{\sigma}^2\otimes\boldsymbol{\sigma}^2 \\ +C_{10}[\mathbf{1}\bar{\otimes}\mathbf{1}+\mathbf{1}\underline{\otimes}\mathbf{1}] & +C_{11}[\boldsymbol{\sigma}\bar{\otimes}\mathbf{1}+\mathbf{1}\underline{\otimes}\boldsymbol{\sigma}] & +C_{12}[\boldsymbol{\sigma}^2\bar{\otimes}\mathbf{1}+\mathbf{1}\underline{\otimes}\boldsymbol{\sigma}^2] \end{bmatrix} \tag{66}$$

Consequently, the tangential stiffness operator of the nonlinear $K-G$ model in Section 2.2.2 forms a very limited subclass as it activates only three out-of the twelve terms in the general framework of incrementally linear hypoelasticity. Under the name of variable moduli models, a good number of simplified hypoelastic material models have proposed and are still used in structural and geotechnical engineering.

(b) Incrementally Nonlinear Hypoelastic Models:
Another rate independent restriction leads to a class of incrementally nonlinear models which have been proposed under the name of hypoplastic models. Because of the incremental nonlinearity they are capable to distinguish between different loading and unloading stiffness properties in analogy to the endochronic time model introduced by K. VALANIS [1975]. In the absence of a loading function, it is understood that the irreversible contribution leads to continuous energy dissipation under repeated load cycles in contrast to unload-reload cycles in elastoplasticity.

# 3 Elastoplastic Models

There are several points of departure to develop a consistent theory for elastoplastic constitutive models. Traditionally we start from the underlying rheological model shown in Figure 6 which lends itself to develop the elastoplastic stress-strain relations for uniaxial conditions. The basic concepts may be generalized using the internal variable theory of COLEMAN & GURTIN [1967] based on continuum thermodynamics which provides an elegant repository for history dependent inelasticity. In the sequel we will confine our discussion to rate independent material behavior. In this case starting point of the internal variable models is the assumption that the stress tensor may be represented as a function of the current strain tensor and a finite number of parameters, $q_1, q_2, ...q_n$.

$$\boldsymbol{\sigma} = \boldsymbol{f}(\boldsymbol{\epsilon}, q_1, q_2, ...q_n) \tag{67}$$

These internal variables $q_1, q_2, ...q_n$ represent the material state that depends on the process history. Their current values is defined in terms of evolution equations which form in general a system of ordinary first order differential equations

$$\dot{q_i}(t) = g_i(\boldsymbol{\sigma}, \boldsymbol{\epsilon}, q_1(t), q_2(t), ..q_n(t)) \quad \text{where} \quad i = 1, 2, ...n \tag{68}$$

The evolution equations specify the temporal change of the internal variables depending on their current value and input histories either in the form of stress or strain control. For strain control, the general integral of the functional

$$q_i(t) = \boldsymbol{\mathcal{F}}_{t_o\le\tau\le t}(\boldsymbol{\epsilon}(\tau), q_1(t_o), q_2(t_o), ..q_n(t_o)) \tag{69}$$

needs to be evaluated numerically. The internal variables represent the memory properties of the inelastic material behavior. Their physical meaning is to represent the dynamical process which take place because of inelasticity at the material microstructure and to make visible their macroscopic effects. In plasticity, they constitute the plastic strain tensor and the reduced variables for isotropic and kinematic hardening. In elastic damage mechanics they form the damage tensor and the scalar damage variables for volumetric and deviatoric elastic stiffness degradation. Thereby, the evolution equations are additional constitutive equations which augment the stress-strain relation.

In the sequel we start from the uniaxial relations of the the rheological model and extend them to triaxial conditions using an engineering approach. For illustration we consider the one-invariant von Mises plasticity model and its extension to the two-invariant DRUCKER-PRAGER [1952] model as well as the three-invariant extension along the line of the five parameter model by WILLAM-WARNKE [1975]. We will conclude this section with the example problem of simple shear which will illustrate the dramatic effect of volumetric-deviatoric interaction on the overall response behavior.

## 3.1 Elastoplastic Rheological Model

The serial arrangement of an elastic spring and a friction element dates back to Reuss who proposed the additive decomposition of strain into elastic and plastic components. The combination of an elastic

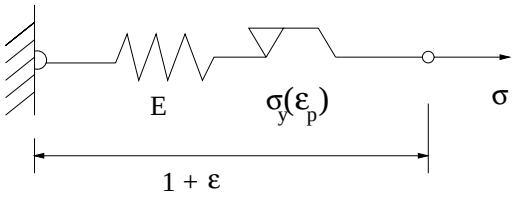


Figure 6: Elastoplastic Serial Model of Spring and Friction Element

spring and the friction element leads to two formats of elastoplasticity, one is the 'Deformation Theory' of Hencky, and the other is the 'Rate Theory' of Prandtl-Reuss. The deformation theory is essentially a secant-type formulation of plasticity along the nonlinear K-G model which is augmented by a plastic load-elastic unload condition. This leads to discontinuities in the transition region from elasticity to plasticity under repeated loading and unloading cycles. Thus, we will concentrate on the flow theory of plasticity, although the continuity leads to overly stiff elastic response predictions when plastic loading takes place to-the-side of a smooth yield surface without corners.

In small deformation problems the flow theory is based on the additive decomposition of the total strain rate into elastic and plastic components,

$$\dot{\epsilon} = \dot{\epsilon}_e + \dot{\epsilon}_p \tag{70}$$

the serial arrangement of an elastic spring and a plastic friction element infers stress equivalence in the two elements. In other terms the state of stress in the elastic spring is limited by the slip conditions of the friction element. The behavior in the elastic response regime $\sigma \leq \sigma_y$ is described by Hooke's law,

$$\dot{\epsilon}_e = \frac{\dot{\sigma}}{E} \tag{71}$$

while the plastic response is active when the stress reaches the yield condition, such that under persistent plastic loading when $\sigma = \sigma_y$

$$\dot{\epsilon}_p = \frac{\dot{\sigma}}{E_p} \tag{72}$$

Consequently,

$$\dot{\epsilon} = \frac{\dot{\sigma}}{E} + \frac{\dot{\sigma}}{E_p} = \frac{\dot{\sigma}}{E_{ep}} \tag{73}$$

with the elastoplastic tangent stiffness

$$E_{ep} = \frac{E\,E_p}{E + E_p} \tag{74}$$

Figure 7 illustrates the elastoplastic response for a load-unload-reload input history. Note that the tangent modulus $E_t = E_{ep}$ may range from positive to negative values according to

$$E_{ep} \begin{cases} > 0, & \text{Hardening} \\ = 0, & \text{Perfectly Plastic} \\ < 0, & \text{Softening} \end{cases}$$

with the understanding that a critical value for softening is reached when $E_p^{crit} = -E$.

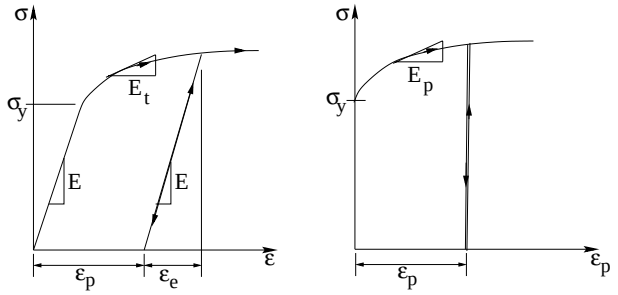


Figure 7: Load-Unload-Reload Response of Elastoplastic Hardening Solid

We also note the indeterminacy of the plastic strain rate for perfectly plastic behavior, when the plastic modulus is zero, $\dot{\epsilon}_p = \frac{0}{0}$. This indicates that strain rather than stress control must be used to maintain uniqueness for elastic-perfectly plastic conditions as well as for strain-softening,

$$\dot{\epsilon}_p = \frac{\dot{\sigma}}{E_p} = \frac{E}{E + E_p}\dot{\epsilon} \tag{75}$$

This assures that the plastic strain rate increases with increasing strain rate and vice versa. Moreover, the intuitive loading condition must be replaced by a more precise yield condition of the form of the scalar-valued yield function of stress

$$F(\sigma) = |\sigma| - \sigma_y = 0 \tag{76}$$

which acts as a threshold condition when the stress demand $|\sigma|$ reaches the yield capacity of the elasto-plastic material. We note that plastic loading requires, (i) the stress path has to reach the yield strength, which is here assumed to be the same in uniaxial tension and compression, and (ii) under persistent plastic action the rate of strain must satisfy $\epsilon\,\dot{\epsilon} > 0$ under strain control.

## 3.2 General Format of the Flow Theory of Elastoplasticity

Starting from the small strain setting, where the strain tensor is the symmetric part of the displacement gradient, $\boldsymbol{\epsilon} = \frac{1}{2}[\nabla \boldsymbol{u} + \nabla^t \boldsymbol{u}]$, the serial arrangement of the rheological model in Figure 6 decomposes the strain into the sum of elastic and plastic parts.

$$\boldsymbol{\epsilon} = \boldsymbol{\epsilon}_e + \boldsymbol{\epsilon}_p \tag{77}$$

1. *Elastic Behavior:*

   Extending the hyperelastic concept of a strain energy potential, we start this time from the free energy function $\Psi$ according to Helmholtz, in which the plastic strains and the internal variable $\kappa$ account for the hardening behavior.

   $$\Psi = \Psi(\boldsymbol{\epsilon}, \boldsymbol{\epsilon}_p, \kappa) \tag{78}$$

   With the classical arguments of Clausius–Duhem, the inequality of the second law of thermodynamics yields the stress tensor $\boldsymbol{\sigma}$ as thermodynamically conjugate variable to the elastic strains,

   $$\boldsymbol{\sigma} = \frac{\partial \Psi}{\partial \boldsymbol{\epsilon}_e} \qquad \text{and} \qquad \dot{\boldsymbol{\sigma}} = \boldsymbol{\mathcal{E}} : [\dot{\boldsymbol{\epsilon}} - \dot{\boldsymbol{\epsilon}}_p] \tag{79}$$

   Thereby the relation between the stress rates and the elastic strain rates is defined in terms of the fourth order elasticity tensor $\boldsymbol{\mathcal{E}}$ discussed earlier on in Section 2.

2. *Plastic Yield Condition:*

   The yield function

   $$F(\boldsymbol{\sigma}, \kappa) = f(\boldsymbol{\sigma}) - r_y(\kappa) \leq 0 \qquad \text{with} \qquad \boldsymbol{n} = \frac{\partial F}{\partial \boldsymbol{\sigma}} \tag{80}$$

   delimits the elastic domain with the normal $\boldsymbol{n}$ to the tangent plane at the yield surface. The geometric interpretation of the yield function in the form of a yield surface helps to visualize the elastic region which may expand or shrink according to the underlying hardening/softening model. Hereby, the yield resistance $r_y$ is conjugate to the internal variable for isotropic hardenening $\kappa$,

   $$r_y = \frac{\partial \Psi}{\partial \kappa} \qquad \text{and} \qquad \dot{r}_y = H_p \, \dot{\kappa}, \tag{81}$$

   Thereby, the relation between the rate of the yield resistance and the hardening variable defines the hardening modulus $H_p$.

3. *Plastic Flow Rule:*

   The evolution of plastic strains is governed by the plastic flow rule,

   $$\dot{\boldsymbol{\epsilon}}_p = \dot{\lambda} \, \boldsymbol{m} \qquad \text{with} \qquad \boldsymbol{m} = \frac{\partial Q}{\partial \boldsymbol{\sigma}} \tag{82}$$

   whereby $\boldsymbol{m}$ denotes the normal to the plastic potential $Q$ which differs from the yield function $F$ in the non–associated case. In the above equation, $\dot{\lambda}$ denotes the plastic multiplier, and $Q = Q(\boldsymbol{\sigma})$ is the plastic flow potential. We speak of associated flow when $\boldsymbol{m} \parallel \boldsymbol{n}$ which infers normality of plastic flow in the direction of the gradient of the yield function. In the case of non-associated flow, $Q \neq F$, one speaks of loss of normality.

4. *Plastic Consistency Condition:*

   For plastic behavior not only the yield condition must hold, $F = 0$, but also the plastic consistency condition must be satisfied under persistent plastic action. The plastic consistency condition of Prager $\dot{F} = 0$ enforces the stress path to remain on the yield surface (at least in the differential sense).

   The set of constitutive equations is completed by the Kuhn–Tucker condition:

$$F \leq 0 \qquad \dot{\lambda} \geq 0 \qquad F\,\dot{\lambda} = 0 \tag{83}$$

   together with the plastic consistency condition:

$$\dot{F} = 0. \tag{84}$$

   From the latter the plastic multiplier results in,

$$\dot{\lambda} = \frac{1}{h_p}\,\boldsymbol{n} : \boldsymbol{\mathcal{E}} : \dot{\boldsymbol{\epsilon}} \quad \text{with} \quad h_p = H_p + \boldsymbol{n} : \boldsymbol{\mathcal{E}} : \boldsymbol{m} \tag{85}$$

5. *Elastoplastic Stiffness Relation:*

   Substituting the plastic multiplier into the elastoplastic stress-strain relation yields:

$$\dot{\boldsymbol{\sigma}} = \boldsymbol{\mathcal{E}} : [\dot{\boldsymbol{\epsilon}} - \dot{\lambda}\boldsymbol{m}] = \boldsymbol{\mathcal{E}} : [\dot{\boldsymbol{\epsilon}} - \boldsymbol{m}\frac{\boldsymbol{n} : \boldsymbol{\mathcal{E}} : \dot{\boldsymbol{\epsilon}}}{H_p + \boldsymbol{n} : \boldsymbol{\mathcal{E}} : \boldsymbol{m}}] \tag{86}$$

   Rearranging results in the elasto–plastic tangent operator $\boldsymbol{\mathcal{E}}_{ep}$ which relates the stress and strain rates

$$\dot{\boldsymbol{\sigma}} = \boldsymbol{\mathcal{E}}_{ep} : \dot{\boldsymbol{\epsilon}} \tag{87}$$

   in the form of a rank–one update of the elastic material operator,

$$\boldsymbol{\mathcal{E}}_{ep} = \boldsymbol{\mathcal{E}} - \frac{1}{h_p}\,\boldsymbol{\mathcal{E}} : \boldsymbol{m} \otimes \boldsymbol{n} : \boldsymbol{\mathcal{E}} = \boldsymbol{\mathcal{E}} - \frac{1}{h_p}\bar{\boldsymbol{m}} \otimes \bar{\boldsymbol{n}} \tag{88}$$

   where $\bar{\boldsymbol{m}} = \boldsymbol{\mathcal{E}} : \boldsymbol{m}$ and $\bar{\boldsymbol{n}} = \boldsymbol{n} : \boldsymbol{\mathcal{E}}$. The update notation emphasizes that the elastic reference tensor is being reduced by the plastic rank-one modification $\bar{\boldsymbol{m}} \otimes \bar{\boldsymbol{n}}$. Note, that the critical softening modulus is reached when $h_p^{crit} = 0$, or in other terms, when $H_p^{crit} = -\boldsymbol{n} : \boldsymbol{\mathcal{E}} : \boldsymbol{m}$. We also note the loss of symmetry, i.e. $\boldsymbol{\mathcal{E}}_{ep} \neq \boldsymbol{\mathcal{E}}_{ep}^t$ for non-associated flow when $\boldsymbol{n} \neq \boldsymbol{m}$.

## 3.3 Special Case of $J_2$-Plasticity

In $J_2$-plasticity we combine the von Mises condition of plastic yielding with the plastic flow rule and the additive decomposition of Prandtl-Reuss. In view of the deviatoric setting of plasticity we may restrict the development of $J_2$-plasticity to a deviatoric stress-strain relation. For the sake of simplicity we describe the resistance of the material by the yield strength in uniaxial tension, $r_y = \sigma_y$, and we assume elastic perfectly plastic behavior to eliminate the need for internal variables to describe hardening/softening.

1. *$J_2$-Yield Function:*

$$F(\boldsymbol{s}) = \frac{1}{2}\boldsymbol{s} : \boldsymbol{s} - \frac{1}{3}\sigma_y^2 = 0 \tag{89}$$

2. *Associated Plastic Flow Rule:*

$$\dot{\boldsymbol{\epsilon}}_p = \dot{\lambda}\, \boldsymbol{s} \quad \text{where} \quad \boldsymbol{m} = \frac{\partial F}{\partial \boldsymbol{s}} = \boldsymbol{s} \tag{90}$$

3. *Plastic Consistency Condition:*

$$\dot{F} = \frac{\partial F}{\partial \boldsymbol{s}} : \dot{\boldsymbol{s}} = \boldsymbol{s} : \dot{\boldsymbol{s}} = 0 \tag{91}$$

The deviatoric stress-strain rates are related by

$$\dot{\boldsymbol{s}} = 2G\,[\dot{\boldsymbol{e}} - \dot{\boldsymbol{e}}_p] = 2G\,[\dot{\boldsymbol{e}} - \dot{\lambda}\boldsymbol{s}] \tag{92}$$

Substituting into the consistency condition

$$\dot{F} = 2G\boldsymbol{s} : [\dot{\boldsymbol{e}} - \dot{\lambda}\boldsymbol{s}] = 0 \tag{93}$$

leads to the plastic multiplier:

$$\dot{\lambda} = \frac{\boldsymbol{s} : \dot{\boldsymbol{e}}}{\boldsymbol{s} : \boldsymbol{s}} \tag{94}$$

4. *Deviatoric Stress-Strain Relation:*

The deviatoric stress-strain rate expression may be written as

$$\dot{\boldsymbol{s}} = 2G\,[\dot{\boldsymbol{e}} - \frac{\boldsymbol{s} : \dot{\boldsymbol{e}}}{\boldsymbol{s} : \boldsymbol{s}}\boldsymbol{s}] = 2G\,[\boldsymbol{\mathcal{I}} - \frac{\boldsymbol{s} \otimes \boldsymbol{s}}{\boldsymbol{s} : \boldsymbol{s}}] : \dot{\boldsymbol{e}} \tag{95}$$

or in short form as

$$\dot{\boldsymbol{s}} = \boldsymbol{\mathcal{G}}_{ep} : \dot{\boldsymbol{e}} \quad \text{whith} \quad \boldsymbol{\mathcal{G}}_{ep} = 2G\,[\boldsymbol{\mathcal{I}} - \frac{\boldsymbol{s} \otimes \boldsymbol{s}}{\boldsymbol{s} : \boldsymbol{s}}] \tag{96}$$

5. *Tangent Stiffness Operator of $J_2$-Elastoplasticity:*

Including the elastic volumetric response, $[tr\dot{\boldsymbol{\sigma}}] = 3K[tr\dot{\boldsymbol{\epsilon}}]$, the elastoplastic stress-strain relationship leads to:

$$\dot{\boldsymbol{\sigma}} = \frac{1}{3}[tr\dot{\boldsymbol{\sigma}}]\mathbf{1} + \dot{\boldsymbol{s}} = K[tr\dot{\boldsymbol{\epsilon}}]\mathbf{1} + \boldsymbol{\mathcal{G}}_{ep} : \dot{\boldsymbol{e}} \tag{97}$$

Considering

$$\dot{\boldsymbol{\sigma}} = K[tr\dot{\boldsymbol{\epsilon}}]\mathbf{1} + \boldsymbol{\mathcal{G}}_{ep} : [\dot{\boldsymbol{\epsilon}} - \frac{1}{3}[tr\dot{\boldsymbol{\epsilon}}]\mathbf{1}] \tag{98}$$

The combined elastoplastic tangent relationship results in

$$\dot{\boldsymbol{\sigma}} = \boldsymbol{\mathcal{E}}_{ep} : \dot{\boldsymbol{\epsilon}} \quad \text{with} \quad \boldsymbol{\mathcal{E}}_{ep} = \Lambda\mathbf{1} \otimes \mathbf{1} + 2G\,[\boldsymbol{\mathcal{I}} - \frac{\boldsymbol{s} \otimes \boldsymbol{s}}{\boldsymbol{s} : \boldsymbol{s}}] \tag{99}$$

which has the same constitutive structure as the nonlinear $K - G$ model in Eq. 54.

## 3.4 Example Problem of Simple Shear

In frictional materials the so-called Reynolds effect of shear dilatancy is one of the central mechanisms which is responsible for the interaction of the volumetric and deviatoric components. In the case of plastic loading the elastoplastic tangential stiffness relationship may be written as

$$\boldsymbol{\mathcal{E}}_{ep} = \boldsymbol{\mathcal{E}} - \frac{1}{h_p}\boldsymbol{\mathcal{R}}_p \quad \text{where} \quad \boldsymbol{\mathcal{R}}_p = \boldsymbol{\mathcal{E}} : \boldsymbol{m} \otimes \boldsymbol{n} : \boldsymbol{\mathcal{E}} \tag{100}$$

Hereby, the plastic dyadic tensor product $\boldsymbol{\mathcal{R}}_p$ is the sole repository of stress- or strain-induced anisotropy and for coupling between the direct and shear behavior in the case of isotropic elasticity.

For definiteness let us examine the relation between shear strains and normal stresses under simple shear, a strain controlled test illustrated in Figure 7. The objective is to determine the source of coupling of the direct stresses and shear strains in the case of elastoplastic formulations of increasing complexity.

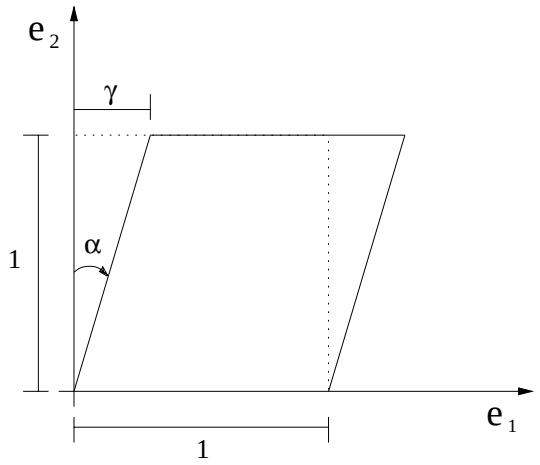


Figure 7: Simple Shear Problem.

Figure 8 illustrates the fundamentally different response predictions of the pressure-independent von Mises and a pressure-sensitive and dilatant two–invariant plasticity formulation in terms of $I_1 = [tr\boldsymbol{\sigma}]$ and $J_2 = \frac{1}{2}[tr\boldsymbol{s}^2]$ as proposed by DRUCKER–PRAGER [1952]. A parabolic generalization of the original two-parameter model may be developed in terms of the friction angle $\alpha_F$ and the cohesive resistance $r_y = \tau_y$ to define the shear strength in the form:

$$F(I_1, J_2) = J_2 + \alpha_F\, I_1 - \tau_y^2 = 0 \tag{101}$$

The two parameters may be identified from uniaxial tension and compression test data $f_t'$ and $f_c'$ as follows

$$\alpha_F = \frac{f_c' - f_t'}{3} \qquad \text{and} \qquad \tau_y^2 = \frac{f_c'\, f_t'}{3} \tag{102}$$

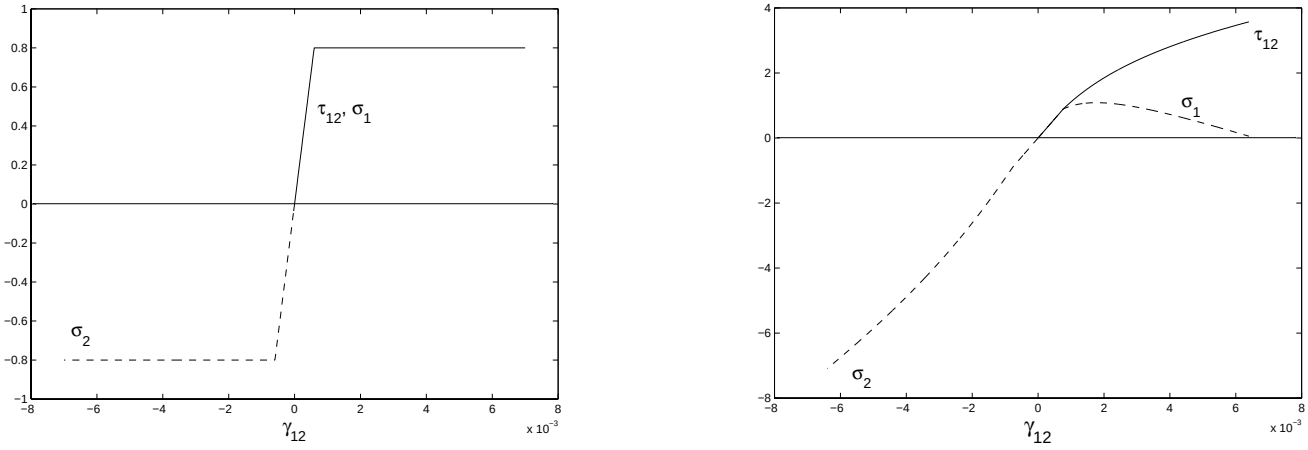


Figure 8: Simple Shear Response Behavior of One-Invariant VON MISES Model (left) and Two-Invariant Parabolic DRUCKER-PRAGER Model (right).

The von Mises yield condition in shear, $\sqrt{J_2} = \tau_y = 0.8\, ksi$ reproduces the elastic-perfectly plastic input, whereby the shear stress-strain relation coincides with the principal stress response. Note, strain control coincides with the stress controlled situation of pure shear, $\tau_{12} = \sigma_1 = -\sigma_2 = \tau_y$ if there is no coupling between the volumetric and deviatoric response behavior. In contrast, the simple shear test exhibits apparent hardening, when an associated flow rule is used in conjunction of the parabolic Drucker-Prager yield condition. Calibration of the two-parameter representation with the uniaxial tensile and compressive strength values $f'_c = 4\, ksi$ and $f'_t = 0.6\, ksi$ leads to the same incipient shear strength as the von Mises model. However, in contrast to the pressure-independent plasticity model, the parabolic Drucker-Prager model exhibits very different behavior in the plastic regime because of the apparent hardening under persistent plastic flow in spite of the underlying assumption of perfectly plastic behavior. We observe a large increase of shear stress, which is accompanied by an equivalent increase of the minor principal stress $-\sigma_2 >> \tau_y$ at the cost of reducing the major principal tensile stress from tension into compression.

In view of these fundamental differences of pressure-sensitive vs pressure-insensitive plasticity models we further investigate the source of these discrepancies. To this end we systematically examine the influence of the three invariants in the plastic yield condition on the simple shear response and the shear dilatancy in particular.

### 3.4.1 *One-Invariant Plasticity Formulation*

To start with, we consider the effect of the second invariant in the yield condition, $F = F(\rho)$, where the deviator $\rho = \sqrt{\boldsymbol{s} : \boldsymbol{s}}$, defines the radial distance of the yield condition from the hydrostatic axis of the cylindrical Haigh-Westergaard coordinates $\xi, \rho, \theta$ of stress. In this case the expression for the gradient of the yield function defines the normal as

$$\boldsymbol{n} = \frac{\partial F}{\partial \boldsymbol{\sigma}} = \frac{\partial F}{\partial \rho}\frac{\partial \rho}{\partial \boldsymbol{\sigma}} = \frac{F_\rho}{\rho}\boldsymbol{s} \quad \text{where} \quad \frac{\partial \rho}{\partial \boldsymbol{\sigma}} = \frac{1}{\rho}\boldsymbol{s} \tag{103}$$

The partial derivative, $F_\rho = \partial F/\partial \rho$, is a positive scalar which determines the magnitude of the normal shown in Figure 9.

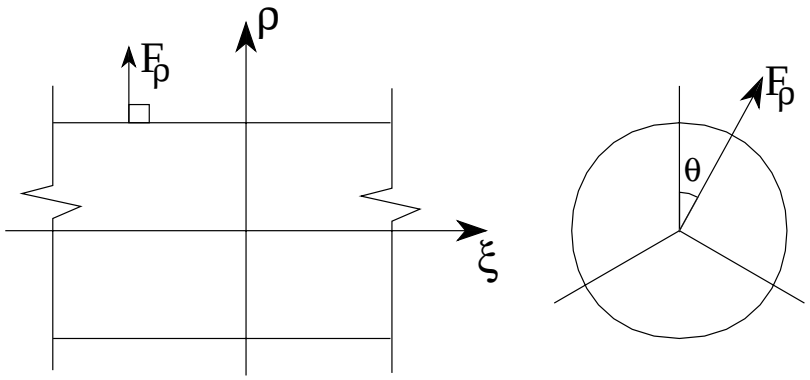


Figure 9: Gradient of Generic Single-Invariant Yield Surface.

The plastic flow direction is defined by the gradient of the plastic potential. In the case of pressure-insensitive plastic flow

$$\boldsymbol{m} = \frac{\partial Q}{\partial \boldsymbol{\sigma}} = \frac{\partial Q}{\partial \rho}\frac{\partial \rho}{\partial \boldsymbol{\sigma}} = \frac{Q_\rho}{\rho}\boldsymbol{s} \tag{104}$$

The expressions for $\boldsymbol{n}$ and $\boldsymbol{m}$ simplify considerably for loading in simple shear when $\dot{\gamma}_{12} > 0$, and when all other strain components remain zero, $\epsilon_{11} = \epsilon_{22} = \epsilon_{33} = \gamma_{23} = \gamma_{13} = 0$. At incipient yielding the elastic shear stress is the only deviatoric component which is non-zero, $s_{12} = \tau_{12} = G\,\gamma_{12}$. With $\rho = \sqrt{\boldsymbol{s} : \boldsymbol{s}} = \sqrt{2}\tau_{12}$, the gradients of the yield function and plastic potential $\boldsymbol{n}$ and $\boldsymbol{m}$ in vector notation reduce to,

$$\boldsymbol{n} = \begin{bmatrix} 0 & 0 & 0 & \frac{1}{\sqrt{2}}F_\rho & 0 & 0 \end{bmatrix}^t \quad \text{and} \quad \boldsymbol{m} = \begin{bmatrix} 0 & 0 & 0 & \frac{1}{\sqrt{2}}Q_\rho & 0 & 0 \end{bmatrix}^t \tag{105}$$

For plastic loading in simple shear the elastoplastic tangent matrix has the simple format:

$$\begin{Bmatrix} \dot{\sigma}_{11} \\ \dot{\sigma}_{22} \\ \dot{\sigma}_{33} \\ \cdots \\ \dot{\tau}_{12} \\ \dot{\tau}_{23} \\ \dot{\tau}_{13} \end{Bmatrix} = \begin{bmatrix} K+\frac{4}{3}G & K-\frac{2}{3}G & K-\frac{2}{3}G & \vdots & 0 & 0 & 0 \\ K-\frac{2}{3}G & K+\frac{4}{3}G & K-\frac{2}{3}G & \vdots & 0 & 0 & 0 \\ K-\frac{2}{3}G & K-\frac{2}{3}G & K+\frac{4}{3}G & \vdots & 0 & 0 & 0 \\ \cdots & \cdots & \cdots & \cdots & \cdots & \cdots & \cdots \\ 0 & 0 & 0 & \vdots & G[1-\frac{1}{2\,h_p}G\,F_\rho Q_\rho] & 0 & 0 \\ 0 & 0 & 0 & \vdots & 0 & G & 0 \\ 0 & 0 & 0 & \vdots & 0 & 0 & G \end{bmatrix} \begin{Bmatrix} 0 \\ 0 \\ 0 \\ \cdots \\ \dot{\gamma}_{12} \\ 0 \\ 0 \end{Bmatrix} \tag{106}$$

For von Mises plasticity the dyadic tensor product adds only a single term to $E^{ep}_{44}$ on the principal diagonal. Note that the off-diagonal partitions of the elastoplastic tangent operator are zero similar to isotropic elasticity exhibiting no coupling between the normal stresses and shear strains and vice versa.

For completeness let us examine under what conditions does the elastoplastic tangent operator $\boldsymbol{E}_{ep}$ become singular. To this end we partition the elastoplastic tangent matrix into the four components and use the Schur theorem of determinants which states

$$\det \boldsymbol{E}_{ep} = \det \boldsymbol{E}_{ss} \det \left( \boldsymbol{E}_{nn} - \boldsymbol{E}_{ns}\boldsymbol{E}^{-1}_{ss}\boldsymbol{E}_{sn} \right) \tag{107}$$

A necessary and sufficient condition for $\det \boldsymbol{E}_{ep} = 0$ is reached, when either $\det \boldsymbol{E}_{ss} = 0$ or when the determinant of the so-called Schur complement is zero, $\det \left( \boldsymbol{E}_{nn} - \boldsymbol{E}_{ns} \boldsymbol{E}_{ss}^{-1} \boldsymbol{E}_{sn} \right) = 0$. In the case of no coupling, $\boldsymbol{E}_{ns} = \boldsymbol{E}_{sn} = \boldsymbol{0}$, and with the positive partition of the elastic stiffness, $\det \boldsymbol{E}_{nn} > 0$, the only possibility that the elastoplastic tangent operator turns singular, arises when $\det \boldsymbol{E}_{ss} = 0$. This condition is true, if and only if the diagonal term vanishes, i.e. $E_{44}^{ep} = 0$. Substituting the normals $\boldsymbol{n}$ and $\boldsymbol{m}$ in Eq. 105 into the denominator $h_p = H_p + \boldsymbol{n} : \boldsymbol{E} : \boldsymbol{m} = H_p + \frac{1}{2} G \, F_\rho Q_\rho$, the pastic degradation of the elastic stiffness results in

$$E_{44}^{ep} = G \left[ 1 - \frac{1}{1 + \frac{2 \, H_p}{G \, F_\rho Q_\rho}} \right] \tag{108}$$

As the shear modulus is strictly positive, $G > 0$, and as $F_\rho Q_\rho > 0$ in the case of the von Mises yield cylinder, the diagonal shear stiffness goes to zero, $E_{44}^{ep} \to 0$, only if the hardening parameter goes to zero, $H_p \to 0$. Consequently,

$$\det \boldsymbol{E}_{ep} = 0 \quad \text{iff} \quad H_p = 0 \tag{109}$$

### 3.4.2 *Two-Invariant Plasticity Formulation*

In the second stage, we examine the dilatational stress relation of a two-invariant Drucker-Prager yield condition, which includes both hydrostatic and deviatoric plastic effects as shown in Figure 10.

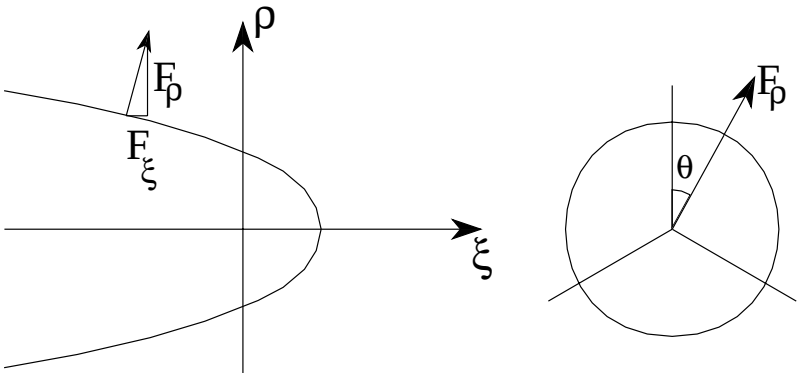


Figure 10: Gradient of Generic Two-Invariant Yield Surface.

The normal gradient of the two-invariant formulation reads in the case of two-invariant plasticity:

$$\boldsymbol{n} = \frac{\partial F}{\partial \boldsymbol{\sigma}} = \frac{\partial F}{\partial \xi} \frac{\partial \xi}{\partial \boldsymbol{\sigma}} + \frac{\partial F}{\partial \rho} \frac{\partial \rho}{\partial \boldsymbol{\sigma}} = \frac{F_\xi}{\sqrt{3}} \boldsymbol{1} + \frac{F_\rho}{\rho} \boldsymbol{s} \tag{110}$$

where $\xi = \frac{1}{\sqrt{3}} \boldsymbol{\sigma} : \boldsymbol{1}$ denotes the dependence on the first stress invariant $I_1 = [tr \boldsymbol{\sigma}]$. The scalar derivative is in this case $F_\xi = \partial F / \partial \xi$, while the tensor derivatives are $\partial \xi / \partial \boldsymbol{\sigma} = \frac{1}{\sqrt{3}} \boldsymbol{1}$.

In analogy to the normal $\boldsymbol{n}$, the gradient of the non-associated plastic potential is expressed as

$$\boldsymbol{m} = \frac{\partial Q}{\partial \boldsymbol{\sigma}} = \frac{\partial Q}{\partial \xi} \frac{\partial \xi}{\partial \boldsymbol{\sigma}} + \frac{\partial Q}{\partial \rho} \frac{\partial \rho}{\partial \boldsymbol{\sigma}} = \frac{Q_\xi}{\sqrt{3}} \boldsymbol{1} + \frac{Q_\rho}{\rho} \boldsymbol{s} \tag{111}$$

In vector form the two gradients read for simple shear:

$$\boldsymbol{n} = \left[\frac{F_\xi}{\sqrt{3}}, \frac{F_\xi}{\sqrt{3}}, \frac{F_\xi}{\sqrt{3}}, \frac{1}{\sqrt{2}}F_\rho, 0, 0\right]^t \quad \text{and} \quad \boldsymbol{m} = \left[\frac{Q_\xi}{\sqrt{3}}, \frac{Q_\xi}{\sqrt{3}}, \frac{Q_\xi}{\sqrt{3}}, \frac{1}{\sqrt{2}}Q_\rho, 0, 0\right]^t \tag{112}$$

The dyadic product $\boldsymbol{\mathcal{R}}_p = \boldsymbol{\mathcal{E}} : \boldsymbol{m} \otimes \boldsymbol{n} : \boldsymbol{\mathcal{E}}$ of the plastic tangent stiffness leads to loss of symmetry if $F_\rho \neq Q_\rho$ or if $F_\xi \neq Q_\xi$.

$$\boldsymbol{R}_p = \left[\begin{array}{ccc:ccc} 3K^2F_\xi Q_\xi & 3K^2F_\xi Q_\xi & 3K^2F_\xi Q_\xi & \sqrt{\frac{3}{2}}K\,G\,F_\rho Q_\xi & 0 & 0 \\ 3K^2F_\xi Q_\xi & 3K^2F_\xi Q_\xi & 3K^2F_\xi Q_\xi & \sqrt{\frac{3}{2}}K\,G\,F_\rho Q_\xi & 0 & 0 \\ 3K^2F_\xi Q_\xi & 3K^2F_\xi Q_\xi & 3K^2F_\xi Q_\xi & \sqrt{\frac{3}{2}}K\,G\,F_\rho Q_\xi & 0 & 0 \\ \hline \sqrt{\frac{3}{2}}K\,G\,F_\xi Q_\rho & \sqrt{\frac{3}{2}}K\,G\,F_\xi Q_\rho & \sqrt{\frac{3}{2}}K\,G\,F_\xi Q_\rho & \frac{1}{2}G^2\,F_\rho Q_\rho & 0 & 0 \\ 0 & 0 & 0 & 0 & 0 & 0 \\ 0 & 0 & 0 & 0 & 0 & 0 \end{array}\right] \tag{113}$$

The hardening parameter in the denominator is comprised of three terms,

$$h_p = H_p + \frac{1}{2}G\,F_\rho Q_\rho + 3K\,F_\xi Q_\xi \tag{114}$$

whereby the third contribution introduces an additional term, which is positive as long as $F_\xi Q_\xi > 0$. As expected, now there is coupling between the normal stresses and the shear strain. This shows that plastic loading in the two-invariant formulation results in normal stresses, which are negative, as long as $F_\rho Q_\xi > 0$ and vice versa $F_\xi Q_\rho > 0$. In other terms, pressure-sensitive plastic loading in simple shear induces compressive confinement in the case of kinematic constraints. Thereby, the volumetric-deviatoric interaction depends to a large extent on the volumetric component of the plastic flow rule, which is positive in the conical region of the plastic potential, and which diminishes to zero, i.e. $Q_\xi \to 0$, when the plastic potential approaches the von Mises condition.

The singularity of the elastoplastic tangent operator $\boldsymbol{E}_{ep}$ is again determined in terms of singular partitions using the Schur theorem of determinants. The diagonal format of the shear partition suggests to examine the diagonal term

$$E^{ep}_{44} = G\left[1 - \frac{1}{1 + \frac{2H_p + 6K\,F_\xi Q_\xi}{G\,F_\rho Q_\rho}}\right] \tag{115}$$

The elastic bulk and shear moduli, $K, G$, and the derivatives $F_\xi$, $F_\rho$, and $Q_\xi, Q_\rho$ are all positive in the conical region of the yield surface and the plastic potential. Consequently, the diagonal term will remain positive, $E^{ep}_{44} > 0$, and the simple shear response exhibits 'apparent' hardening in the case of perfectly plastic behavior, when $H_p = 0$. The tangent operator becomes singular only when the plastic modulus reaches the limiting softening value

$$H_p^{limit} = -3K\,F_\xi Q_\xi \tag{116}$$

In summary, softening is needed to compensate for the apparent hardening effect of the volumetric dependence of the yield function and the plastic potential. Thereby, the singularity depends critically on the volumetric components of the yield condition and the plastic potential , i.e. $H_p \to 0$ as $F_\xi Q_\xi \to 0$.

### 3.4.3 Three-Invariant Plasticity Formulation

In the third and final study we generalize the plasticity formulation and include the effect of the third invariant in the yield function and the plastic potential. The effect of the third invariant leads to the triple-symmetric shape of the yield function in the deviatoric plane as illustrated in Figure 11.

In this case the gradient operators are becoming considerably more involved in view of the definition of the third invariant, which is here expressed in terms of the angle of similarity

$$\theta = \frac{1}{3} cos^{-1}[\frac{3\sqrt{3}J_3}{2J_2^{1.5}}] \tag{117}$$

where $J_3 = \det \boldsymbol{s}$.

The gradients $\boldsymbol{n}, \boldsymbol{m}$ are comprised of three contributions, i.e.

$$\boldsymbol{n} = \frac{\partial F}{\partial \boldsymbol{\sigma}} = \frac{\partial F}{\partial \xi}\frac{\partial \xi}{\partial \boldsymbol{\sigma}} + \frac{\partial F}{\partial \rho}\frac{\partial \rho}{\partial \boldsymbol{\sigma}} + \frac{\partial F}{\partial \theta}\frac{\partial \theta}{\partial \boldsymbol{\sigma}} = \frac{F_\xi}{\sqrt{3}}\mathbf{1} + \frac{F_\rho}{\rho}\boldsymbol{s} + F_\theta \frac{\partial \theta}{\partial \boldsymbol{\sigma}} \tag{118}$$

and

$$\boldsymbol{m} = \frac{\partial Q}{\partial \boldsymbol{\sigma}} = \frac{\partial Q}{\partial \xi}\frac{\partial \xi}{\partial \boldsymbol{\sigma}} + \frac{\partial Q}{\partial \rho}\frac{\partial \rho}{\partial \boldsymbol{\sigma}} + \frac{\partial Q}{\partial \theta}\frac{\partial \theta}{\partial \boldsymbol{\sigma}} = \frac{Q_\xi}{\sqrt{3}}\mathbf{1} + \frac{Q_\rho}{\rho}\boldsymbol{s} + Q_\theta \frac{\partial \theta}{\partial \boldsymbol{\sigma}} \tag{119}$$

The additional scalar derivatives include $F_\theta = \frac{\partial F}{\partial \theta}$ and $Q_\theta = \frac{\partial Q}{\partial \theta}$, while the tensor derivative is complicated, as

$$\frac{\partial \theta}{\partial \boldsymbol{\sigma}} = \frac{\sqrt{3}}{2\sqrt{1-\cos^2 3\theta}}\left[\frac{1}{J_2^{1.5}}\frac{\partial J_3}{\partial \boldsymbol{\sigma}} - \frac{3J_3}{2J_2^{2.5}}\frac{\partial J_2}{\partial \boldsymbol{\sigma}}\right] \quad \text{with} \quad \frac{\partial J_3}{\partial \boldsymbol{\sigma}} = \boldsymbol{s}\cdot\boldsymbol{s} - \frac{2}{3}J_2\mathbf{1} \quad \text{and} \quad \frac{\partial J_2}{\partial \boldsymbol{\sigma}} = \boldsymbol{s} \tag{120}$$

In vector form the gradients for simple shear appear as:

$$\boldsymbol{n} = \left[\frac{F_\xi}{\sqrt{3}} + \frac{F_\theta}{2\sqrt{3}\tau_{12}}, \frac{F_\xi}{\sqrt{3}} + \frac{F_\theta}{2\sqrt{3}\tau_{12}}, \frac{F_\xi}{\sqrt{3}} - \frac{F_\theta}{\sqrt{3}\tau_{12}}, \frac{1}{\sqrt{2}}F_\rho, 0, 0\right]^t \tag{121}$$

and

$$\boldsymbol{m} = \left[\frac{Q_\xi}{\sqrt{3}} + \frac{Q_\theta}{2\sqrt{3}\tau_{12}}, \frac{Q_\xi}{\sqrt{3}} + \frac{Q_\theta}{2\sqrt{3}\tau_{12}}, \frac{Q_\xi}{\sqrt{3}} - \frac{Q_\theta}{\sqrt{3}\tau_{12}}, \frac{1}{\sqrt{2}}Q_\rho, 0, 0\right]^t \tag{122}$$

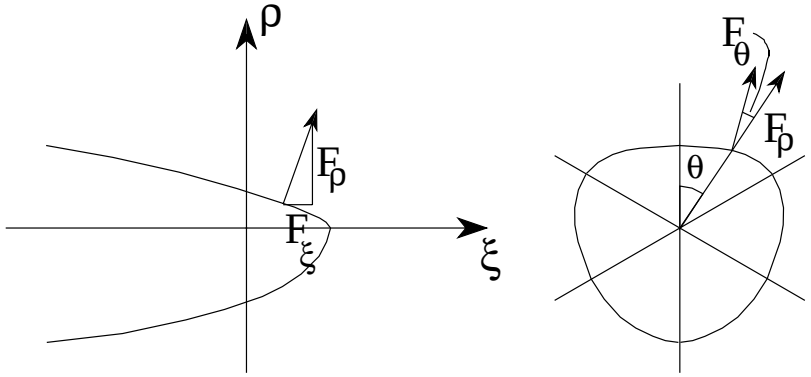


Figure 11: Gradients of Generic Three-Invariant Yield Surface.

In short, the plastic contributions of the third invariant enter the dyadic product $\boldsymbol{\mathcal{R}}_p = \boldsymbol{\mathcal{E}} : \boldsymbol{m} \otimes \boldsymbol{n} : \boldsymbol{\mathcal{E}}$ affecting the coupling partitions $\boldsymbol{\mathcal{R}}^p_{ns}$ and $\boldsymbol{\mathcal{R}}^p_{sn}$ as well as the direct partition $\boldsymbol{\mathcal{R}}^p_{nn}$. To understand their effect we study the individual terms in the different $3 \times 3$ partitions below,

$$\boldsymbol{R}^p_{nn} = \begin{bmatrix} R^p_{11} & R^p_{12} & R^p_{13} \\ R^p_{21} & R^p_{22} & R^p_{23} \\ R^p_{31} & R^p_{32} & R^p_{33} \end{bmatrix} \tag{123}$$

where

$$R^p_{11} = R^p_{22} = R^p_{12} = R^p_{21} = 3\,K^2\,F_\xi Q_\xi + \frac{G^2\,F_\theta\,Q_\theta}{3\tau^2_{12}} + \frac{K\,G}{\tau_{12}}(F_\theta\,Q_\xi + F_\xi\,Q_\theta) \tag{124}$$

$$R^p_{33} = 3\,K^2\,F_\xi Q_\xi + \frac{4G^2\,F_\theta\,Q_\theta}{3\tau^2_{12}} - \frac{2K\,G}{\tau_{12}}(F_\theta\,Q_\xi + F_\xi\,Q_\theta) \tag{125}$$

$$R^p_{13} = R^p_{23} = 3\,K^2\,F_\xi Q_\xi - \frac{2G^2\,F_\theta\,Q_\theta}{3\tau^2_{12}} + \frac{K\,G}{\tau_{12}}(F_\xi\,Q_\theta - 2F_\theta\,Q_\xi) \tag{126}$$

$$R^p_{31} = R^p_{32} = 3\,K^2\,F_\xi Q_\xi - \frac{2G^2\,F_\theta\,Q_\theta}{3\tau^2_{12}} + \frac{K\,G}{\tau_{12}}(F_\theta\,Q_\xi - 2F_\xi\,Q_\theta) \tag{127}$$

The individual terms indicate that the dependence on the third invariant, $F_\theta\,Q_\theta$, introduces different terms in the in-plane and out-of-plane stiffness contributions as opposed to the dependence on the first invariant,$F_\xi\,Q_\xi$. In contrast, the shear partition maintains the same format as the two-invariant model,

$$\boldsymbol{R}^p_{ss} = \begin{bmatrix} \frac{1}{2}G^2\,F_\rho\,Q_\rho & 0 & 0 \\ 0 & 0 & 0 \\ 0 & 0 & 0 \end{bmatrix} \tag{128}$$

The coupling partitions exhibit a distinct difference between in-plane and out-of-plane stiffness contributions in simple shear,

$$\boldsymbol{R}^p_{ns} = \begin{bmatrix} \sqrt{\frac{3}{2}}K\,G\,F_\rho Q_\xi + \frac{G^2}{\sqrt{6}}\frac{F_\rho Q_\theta}{\tau_{12}}, & 0, & 0 \\ \sqrt{\frac{3}{2}}K\,G\,F_\rho Q_\xi + \frac{G^2}{\sqrt{6}}\frac{F_\rho Q_\theta}{\tau_{12}}, & 0, & 0 \\ \sqrt{\frac{3}{2}}K\,G\,F_\rho Q_\xi - \frac{2G^2}{\sqrt{6}}\frac{F_\rho Q_\theta}{\tau_{12}}, & 0, & 0 \end{bmatrix} \tag{129}$$

and

$$\boldsymbol{R}^p_{sn} = \frac{1}{2}\begin{bmatrix} \sqrt{\frac{3}{2}}K\,G\,F_\xi Q_\rho + \frac{G^2}{\sqrt{6}}\frac{Q_\rho F_\theta}{\tau_{12}}, & 0, & 0 \\ \sqrt{\frac{3}{2}}K\,G\,F_\xi Q_\rho + \frac{G^2}{\sqrt{6}}\frac{Q_\rho F_\theta}{\tau_{12}}, & 0, & 0 \\ \sqrt{\frac{3}{2}}K\,G\,F_\xi Q_\rho - \frac{2G^2}{\sqrt{6}}\frac{Q_\rho F_\theta}{\tau_{12}}, & 0, & 0 \end{bmatrix}^t \tag{130}$$

We note that the entries of the dyadic product are no longer the same as in the two-invariant formulation. In fact, the negative sign in the third entry introduces additional structure and distinguishes in-plane from out-of-plane action, which reduces significantly the out-of-plane confining stress $\sigma_{33}$ under simple shear. We also observe the loss of symmetry in all partitions except for the shear partition, when the plastic dilatancy differs from the frictional resistance of the yield condition, $Q_\xi \neq F_\xi$. It might surprise

that the shear partition $\boldsymbol{R}^p_{ss}$ remains unchanged except for the denominator $h_p$ which is augmented by an apparent hardening term from the contribution of the third invariant, i.e.

$$h_p = H_p + \frac{1}{2}G\,F_\rho Q_\rho + 3K\,F_\xi Q_\xi + \frac{3}{2}K\frac{F_\theta Q_\theta}{\tau_{12}^2} \tag{131}$$

Analysis of the singularity in simple shear leads to the question, when does the diagonal term vanish, i.e. $E^{ep}_{44} \to 0$. The answer follows the previous argument of the two invariant formulation. In fact, $\det \boldsymbol{E}_{ep} = 0$ when the plastic softening modulus reaches the limiting value,

$$H_p^{limit} = -3K\left[F_\xi Q_\xi + \frac{1}{2}\frac{F_\theta Q_\theta}{\tau_{12}^2}\right] \tag{132}$$

This indicates that dependence on the third invariant further stabilizes the elastoplastic tangent operator beyond the limit point condition of the two-invariant format.

## 3.5 Concrete Plasticity Model

To illustrate the observations above we resort to numerical simulation of the simple shear test with the help of the three-invariant plasticity model by KANG & WILLAM [1999]. In this case, the curvilinear loading surface $F(\xi, \rho, \theta, q_h, q_s) = 0$, is $C^1$-continuous except at the vertex in equitriaxial tension, see Figure 12a. The triaxial concrete model exhibits pressure-sensitivity of the deviatoric strength as a function of the third stress invariant, inelastic dilatancy during shearing, and brittle-ductile transition from fragile behavior in tension to ductile behavior with increasing confinement.

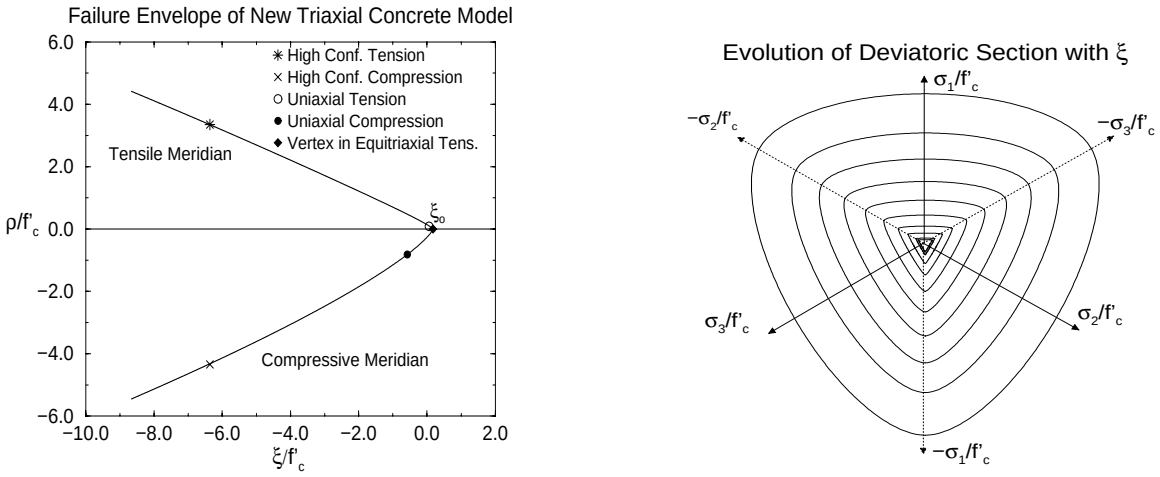


Figure 12: (a) Tension and Compression Meridians, (b) Deviatoric Contours of Triaxial Concrete Envelope, KANG & WILLAM [1999].

The plastic loading function is comprised of three components, the triaxial failure envelope, and a hardening or softening contributions, which are mobilized alternatively in the pre- and post-peak regions:

$$F(\xi, \rho, \theta, q_h, q_s) = F(\xi, \rho, \theta)_{\text{fail}} \;+\; F(\xi, \rho, \theta, k(q_h))_{\text{hardg}} \;+\; F(\xi, \rho, \theta, c(q_s))_{\text{softg}} \tag{133}$$

The failure envelope

$$F(\xi,\rho,\theta)_{\text{fail}} = \frac{\rho r(\theta,e)}{f_c'} - \frac{\rho_1}{f_c'}\left[\frac{\xi-\xi_o}{\xi_1-\xi_o}\right]^{\alpha} = 0 \tag{134}$$

fixes the triaxial strength in stress space in terms of a curvilinear triple-symmetric cone. Figure 12 (a) depicts the failure envelope in terms of the meridians in triaxial compression and extension, and (b) in terms of the deviatoric traces at different levels of hydostatic stress.

The simple shear response is shown in Figure 13 for the three-invariant concrete model. In comparison to the two-invariant formulation shown in Figure 8b, the shear strength and shear ductility are reduced, because of the diminished out-of-plane confinement of the three-invariant model.

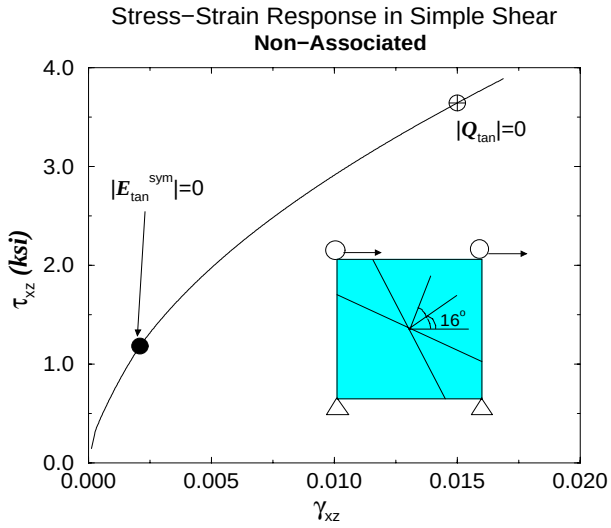


Figure 13: Simple Shear Response of Three-Invariant Concrete Model, KANG & WILLAM [1999].

Note:

The non-associated plasticity model exhibits loss of stability $(\det \boldsymbol{\mathcal{E}}_{ep}^{sym} = \det \boldsymbol{\mathcal{E}}_{tan}^{sym} = 0)$ and discontinuous bifurcation in the form of localized failure $(\det \boldsymbol{Q}_{ep} = \det \boldsymbol{Q}_{tan} = 0)$ in the apparent hardening regime before a limit point condition is reached. For an understanding of the different failure diagnostics the reader is referred to Section 4 and to Appendix II for additional comments on elastoplastic failure in plane strain.

# 4 Analysis of Material Failure

In this section we examine different criteria for initiating failure at the constitutive level of materials. The traditional approach in strength of materials is to probe demand versus resistance with the aid of a limit state condition. This leads to the geometrical visualization of the triaxial state of stress and its proximity to the envelope condition according to OTTO MOHR [1835-1918].

Note: The geometrical interpretation of the triaxial strength hypothesis $F = F(\boldsymbol{\sigma}) = 0$ leads to a critical combination of normal and shear tractions $\sigma, \sigma_T$ on a critical failure plane $\pm\theta$ which

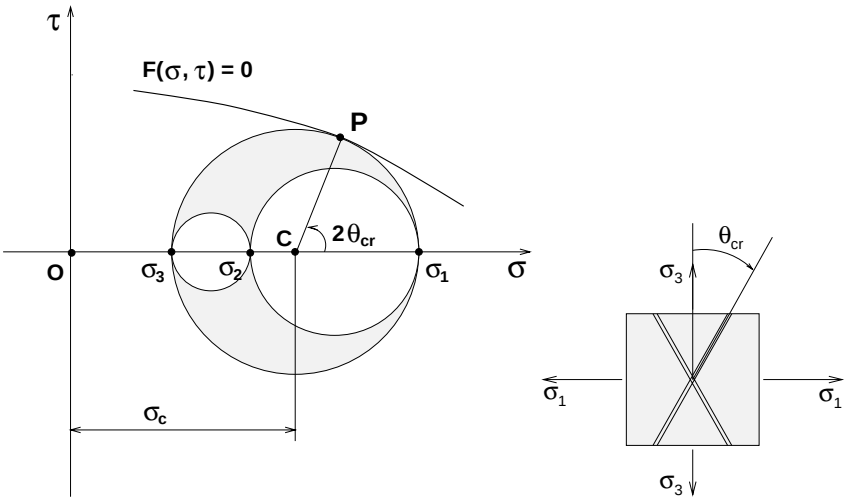


Figure 13 MOHR Concept of Universal Failure Envelope

determines the mode of failure. Thereby the Mohr envelope criterion does not only tell us when failure takes place, but also what kind of failure mode develops. The main draw-back is that it does not depend on the intermediate principal stress since the major principal circle is governed by the maximum and minimum values of stress, $R_{max} = \frac{1}{2}|\sigma_1 - \sigma_3|$. Representative strength criteria for cohesive-frictional materials include the maximum shear stress conditions of MOHR-COULOMB, TRESCA, and LEON, as well as the maximum normal stress condition of RANKINE for tensile cracking. Alternatively to strength of materials, failure has also been described by deformation hypotheses $F(\boldsymbol{\epsilon}) = 0$ such as the SAINT VENANT criterion of maximum normal strain for tensile cracking. Moreover, energy criteria $F(\boldsymbol{\sigma} : \boldsymbol{\epsilon}) = 0$ have been proposed to describe material failure such as the BELTRAMI condition of maximum strain energy and the HUBER criterion of maximum distortional energy. In fact, fracture criteria of a critical stress intensity factor or an equivalent strain energy release rate may also be included in this list of failure criteria, $F(K_I, K_{II}, K_{III}) = 0$ and $F(G_f) = 0$, though discrete fracture mechanics normally starts from the existence of a crack or a notched defect, and defines crack propagation in terms of fracture concepts. In this sense, failure criteria differ from fracture criteria in a fundamental fashion, the former indicate initiation while the latter monitor propagation.

In the original envelope concept of O. Mohr the actual mechanism behind material failure was left open in terms of its kinematic or static manifestation. There was the conceptual distinction between tensile cracking and separation of material interfaces in mode I, and frictional slip among adjacent material interfaces in mode II. However, nothing was said about what happens after failure initiates. In fact, failure initiation was assumed to be critical and trigger collapse of the entire structure.

In view of recent progress in localization analysis it is important to keep in mind that failure is a process of events, which start small at the material level, and which leads to progressive deterioration of the continuum into a discontinuum. Figure 14 illustrates thow his process leads to a progression of kinematic deterioration. It initiates in the form of diffuse failure, and leads through localized, weakly

discontinuous failure to discrete, or strongly discontinuous failure. The following discussion will be restricted to the first two stages of failure, whereby diffuse failure is characterized by loss of material stability and loss of uniqueness, while localized failure results in the formation of weak discontinuities, which signal the onset of kinematic degradation of the continuum into a discontinuum synonymous with loss of ellipticity.

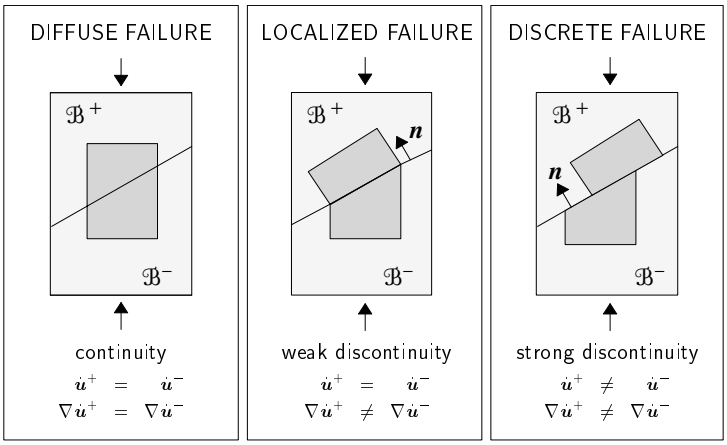


Figure 14: Kinematic Deterioration of the Continuum into a Discontinuum

## 4.1 Loss of Stability–Material Instability

The loss of material stability was identified early on by D. Drucker and R. Hill with the loss of positive internal work. In fact, the exclusion functional of positive second order work density,

$$d^2W = \frac{1}{2}\dot{\boldsymbol{\sigma}} : \dot{\boldsymbol{\epsilon}} = \frac{1}{2}\dot{\boldsymbol{\epsilon}} : \boldsymbol{\mathcal{E}}_t : \dot{\boldsymbol{\epsilon}} > 0, \forall \dot{\boldsymbol{\epsilon}} \neq 0 \tag{135}$$

is widely accepted as a sufficient condition for material stability.

In the case of non-associated elastoplasticity, where $\boldsymbol{\mathcal{E}}_{ep} \neq \boldsymbol{\mathcal{E}}_{ep}{}^t$ this criterion leads to

$$d^2W = \frac{1}{2}\dot{\boldsymbol{\epsilon}} : \boldsymbol{\mathcal{E}}_{ep} : \dot{\boldsymbol{\epsilon}} = \frac{1}{4}\dot{\boldsymbol{\epsilon}} : [\boldsymbol{\mathcal{E}}_{ep} + \boldsymbol{\mathcal{E}}_{ep}^t] : \dot{\boldsymbol{\epsilon}} = \frac{1}{2}\dot{\boldsymbol{\epsilon}} : \boldsymbol{\mathcal{E}} : \dot{\boldsymbol{\epsilon}} - \frac{1}{4h_p}\dot{\boldsymbol{\epsilon}} : [\bar{\boldsymbol{m}} \otimes \bar{\boldsymbol{n}} + \bar{\boldsymbol{n}} \otimes \bar{\boldsymbol{m}}] : \dot{\boldsymbol{\epsilon}} \tag{136}$$

In this context, it is important to recall, that the energy functional extracts only the symmetric part of the tangent operator which leads to the following observation based on the Bromwich eigenvalue bounds of non-symmetric matrices:

$$\lambda_{min}(\boldsymbol{\mathcal{E}}_{ep}^{sym}) \leq \Re(\lambda_{min}(\boldsymbol{\mathcal{E}}_{ep})).. \leq \lambda_{max}(\boldsymbol{\mathcal{E}}_{ep}^{sym}) \tag{137}$$

In other terms, the instability argument coincides with the loss of positive definiteness of the symmetric material operator,

$$\det \boldsymbol{\mathcal{E}}_{ep}^{sym} \stackrel{!}{=} 0 \qquad \rightarrow \qquad \lambda_{min}(\boldsymbol{\mathcal{E}}_{ep}^{sym}) = 0 \tag{138}$$

This argument leads to the critical value of plastic hardening for stability, see MAIER & HUECKL [1979]:

$$H_p^{stabil} = \frac{1}{2}\left[\sqrt{(\boldsymbol{n} : \boldsymbol{\mathcal{E}}_o : \boldsymbol{n})(\boldsymbol{m} : \boldsymbol{\mathcal{E}}_o : \boldsymbol{m})} - \boldsymbol{n} : \boldsymbol{\mathcal{E}}_o : \boldsymbol{m}\right] \tag{139}$$

Therefore, the sufficient condition for stability may be turned around into a upper bound argument of loss of stability in terms of the maximum plastic modulus $H_p^{stabil} \geq H_p^{limit}$.

## 4.2 Diffuse Failure – Loss of Uniqueness

According to Figure 14, diffuse failure maintains continuity in the rate of displacement and the displacement gradient fields. It corresponds to a stationary stress state which defines a limit point on the response path of the material:

$$\dot{\boldsymbol{\sigma}} = \boldsymbol{0} \tag{140}$$

For incrementally linear materials with $\dot{\boldsymbol{\sigma}} = \boldsymbol{\mathcal{E}}_t : \dot{\boldsymbol{\epsilon}}$, this infers that,

$$\boldsymbol{\mathcal{E}}_t : \dot{\boldsymbol{\epsilon}} = \boldsymbol{0} \tag{141}$$

Thus the condition for the loss of uniqueness is equivalent to a singular behavior of the tangent operator $\boldsymbol{\mathcal{E}}_t$,

$$\det \boldsymbol{\mathcal{E}}_t \stackrel{!}{=} 0 \qquad \rightarrow \qquad \lambda_{min}(\boldsymbol{\mathcal{E}}_t) = 0 \tag{142}$$

Recall, that the elastoplastic tangent operator involves a rank–one (rank–two for pressure sensitive plasticity) update of the elastic material operator,

$$\boldsymbol{\mathcal{E}}_{ep} = \boldsymbol{\mathcal{E}} - \frac{1}{h_p}\bar{\boldsymbol{m}} \otimes \bar{\boldsymbol{n}} \tag{143}$$

whereby the update tensors are defined as follows:

$$\begin{aligned} \bar{\boldsymbol{m}} &= \boldsymbol{\mathcal{E}} : \boldsymbol{m} \\ \bar{\boldsymbol{n}} &= \boldsymbol{n} : \boldsymbol{\mathcal{E}} \end{aligned} \tag{144}$$

Pre–conditioning of the elasto–plastic tangent operator with the inverse elasticity tensor the following relation appears.

$$\boldsymbol{\mathcal{E}}^{-1} : \boldsymbol{\mathcal{E}}^{ep} = \boldsymbol{\mathcal{I}} - \boldsymbol{\mathcal{E}}^{-1} : \frac{\bar{\boldsymbol{m}} \otimes \bar{\boldsymbol{n}}}{h_p} \tag{145}$$

Due to the rank–one update structure of the elasto–plastic tangent operator, the critical eigenvalue $\lambda_{min}$ of the generalized eigenvalue problem may be evaluated in closed form. This motivates the introduction of the scalar–valued measure of material integrity $d_{\mathcal{E}}$,

$$\lambda_{min}\left(\boldsymbol{\mathcal{E}}^{-1} : \boldsymbol{\mathcal{E}}^{ep}\right) = 1 - d_{\mathcal{E}} \qquad \text{with} \qquad d_{\mathcal{E}} := \frac{\boldsymbol{n} : \boldsymbol{\mathcal{E}} : \boldsymbol{m}}{H_p + \boldsymbol{n} : \boldsymbol{\mathcal{E}} : \boldsymbol{m}}. \tag{146}$$

From the above definition, a necessary condition for loss of uniqueness leads to the critical hardening modulus $H_p^{limit} = 0$ associated with full loss of integrity,

$$1 - d_{\mathcal{E}} \stackrel{!}{=} 0 \tag{147}$$

The criterion presented above can only be understood as a necessary condition for the loss of uniqueness. For non–symmetric elasto–plastic tangent operators, which arise in non–associated plasticity formulations, loss of stability in the form of $\det \boldsymbol{\mathcal{E}}_{ep}^{sym} \stackrel{!}{=} 0$, provides a lower bound condition according to the Bromwich bounds. Consequently, loss of stability which is synonymous with a singularity of the symmetric tangent operator, takes place before the limit point condition in Eq.(142) is reached.

## 4.3 Localized Failure – Loss of Ellipticity

The localization condition is based on the early works of J. HADAMARD and R. HILL. In contrast to the diffuse failure mode described in the previous section, localized failure of weak discontinuities is characterized through a discontinuity in the rate of the displacement gradient, while the field of the displacement rate itself is still continuous. According to the Maxwell compatibility condition, the jump in the rate of the displacement gradient may be expressed in terms of a scalar–valued jump amplitude $\alpha$, the unit jump vector $\boldsymbol{M}$ and the unit normal vector to the discontinuity surface $\boldsymbol{N}$ shown in Figure 14.

$$[|\nabla \dot{\boldsymbol{u}}|] = \alpha\ \boldsymbol{M} \otimes \boldsymbol{N} \qquad \rightarrow \qquad [|\dot{\boldsymbol{\epsilon}}|] = \alpha\ [\ \boldsymbol{M} \otimes \boldsymbol{N}\ ]^{sym} \tag{148}$$

Equilibrium along the discontinuity surface requires that the traction vectors are equal and opposite on both sides of the discontinuity

$$\left[|\dot{\boldsymbol{t}}|\right] = \dot{\boldsymbol{t}}^{+} - \dot{\boldsymbol{t}}^{-} = \boldsymbol{0} \tag{149}$$

According to Cauchy's theorem, we have

$$\left[|\dot{\boldsymbol{t}}|\right] = \boldsymbol{N} \cdot [|\dot{\boldsymbol{\sigma}}|] = \boldsymbol{N} \cdot [|\boldsymbol{\mathcal{E}}_t : \dot{\boldsymbol{\epsilon}}|] = \boldsymbol{0} \tag{150}$$

With the assumption of a linear comparison solid, $[|\boldsymbol{\mathcal{E}}_t|] = \boldsymbol{\mathcal{E}}_t^{+} - \boldsymbol{\mathcal{E}}_t^{-} = \boldsymbol{0}$, the localization condition may be expressed in the form of an eigenvalue problem,

$$\alpha\ \boldsymbol{Q}_t \cdot \boldsymbol{M} = \boldsymbol{0} \qquad \text{with} \qquad \boldsymbol{Q}_t = \boldsymbol{N} \cdot \boldsymbol{\mathcal{E}}_t \cdot \boldsymbol{N} \tag{151}$$

whereby $\boldsymbol{Q}_t$ denotes the tangential localization tensor. The necessary condition for the onset of localization is thus characterized through the singularity of the localization tensor which happens to coincide with the acoustic tensor in wave propagation.

$$\det \boldsymbol{Q}_t \stackrel{!}{=} 0 \qquad \rightarrow \qquad \lambda_{min}(\boldsymbol{Q}_t) = 0 \tag{152}$$

The elasto–plastic localization tensor may be expressed as a rank–one update of the elastic acoustic tensor

$$\boldsymbol{Q}_{ep} = \boldsymbol{Q} - \frac{1}{h_p} \boldsymbol{e}_m \otimes \boldsymbol{e}_n \tag{153}$$

whereby the following abbreviations have been introduced for the update vectors $\boldsymbol{e}_m$ and $\boldsymbol{e}_n$.

$$\begin{aligned} \boldsymbol{e}_m &= \boldsymbol{N} \cdot \boldsymbol{\mathcal{E}} : \boldsymbol{m} \\ \boldsymbol{e}_n &= \boldsymbol{n} : \boldsymbol{\mathcal{E}} \cdot \boldsymbol{N} \end{aligned} \tag{154}$$

Instead of probing the lowest eigenvalue of the localization tensor Eq.(152), we resort to the generalized eigenvalue problem $\det[\boldsymbol{Q}^{-1} \cdot \boldsymbol{Q}^{ep}] \stackrel{!}{=} 0$ in order to detect whether the localization tensor turns singular, see Ottosen & Runesson [1991]. Pre–conditioning of the elasto–plastic acoustic tensor with the inverse of the elastic acoustic tensor leads to:

$$\boldsymbol{Q}^{-1} \cdot \boldsymbol{Q}_{ep} = \boldsymbol{1} - \boldsymbol{Q}^{-1} \cdot \frac{\boldsymbol{e}_m \otimes \boldsymbol{e}_n}{h_p} \tag{155}$$

The closed form solution for the lowest eigenvalue $\lambda_{min}$ introduces a scalar–valued measure of integrity with respect to localization in the form of

$$\lambda_{min}\left(\boldsymbol{Q}^{-1} \cdot \boldsymbol{Q}_{ep}\right) = 1 - d_Q \qquad \text{with} \qquad d_Q = \frac{\boldsymbol{e}_n \cdot \boldsymbol{Q}^{-1} \cdot \boldsymbol{e}_m}{H_p + \boldsymbol{n} : \boldsymbol{\mathcal{E}} : \boldsymbol{m}} \tag{156}$$

It defines a necessary condition for localization as well as the critical hardening modulus $H_p^{loc}$ indicating loss of ellipticity, when

$$1 - d_Q \stackrel{!}{=} 0 \qquad \rightarrow \qquad H_p^{loc} = \boldsymbol{e}_n \cdot \boldsymbol{Q}^{-1} \cdot \boldsymbol{e}_m - \boldsymbol{n} : \boldsymbol{\mathcal{E}} : \boldsymbol{m} \tag{157}$$

For non–symmetric elasto–plastic tangent operators in non–associated plasticity, loss of strong ellipticity in terms of a vanishing determinant of the symmetric part of the tangent acoustic operator, $\det \boldsymbol{Q}_{ep}^{sym} \leq \det \boldsymbol{Q}_{ep} \stackrel{!}{=} 0$, provides a lower bound condition according to the Bromwich theorem. Consequently, loss of strong ellipticity, which is synonymous with a singularity of the symmetric localization operator may take place before the limit point condition Eq.(142) is reached. But most importantly, the critical hardening modulus for localization may still be positive, compare Rudnicki&Rice [1975] before a limit point is reached because of the symmetric features of the second order localization tensor when compared to the fourth order material tensor.

## 4.4 Geometric Localization Condition

The analytical localization condition Eq.(152) may be illustrated geometrically in the form of an envelope condition in analogy to the contact condition of O. Mohr. In the case of the two-invariant plasticity model the localization condition plots as an ellipse in the $\sigma - \sigma_T$ Mohr coordinates. The localization envelope was developed by Benallal&Comi [1996] for elasto–plastic material models.

In the following, the geometric localization format will be established reproducing some results from Kuhl, Ramm & Willam [2000] to illustrate the model problem of simple shear. To this end we briefly summarize the basic ideas of the geometric localization analysis for the non–associated parabolic Drucker–Prager model introduced in the previous section. Eq.(157) indicates the onset of localization when,

$$H_p^{loc} + \boldsymbol{n} : \boldsymbol{\mathcal{E}} : \boldsymbol{m} = \boldsymbol{e}_n \cdot \boldsymbol{Q}^{-1} \cdot \boldsymbol{e}_m \tag{158}$$

Herein, $\boldsymbol{\mathcal{E}}$ denotes the fourth order elasticity tensor, while $\boldsymbol{Q}^{-1}$ is the inverse of the elastic acoustic tensor which can be determined analytically.

$$\begin{aligned} \boldsymbol{\mathcal{E}} &= \Lambda \ \mathbf{1}\otimes\mathbf{1} + 2G \ \boldsymbol{\mathcal{I}} \\ \boldsymbol{Q}^{-1} &= \frac{1}{G} \ \mathbf{1} - \frac{1}{2G\,[1-\nu]} \ \boldsymbol{N}\otimes\boldsymbol{N} \end{aligned} \tag{159}$$

In the following, the localization condition Eq.(158) is recast in the Mohr coordinates $\sigma$ and $\sigma_T$,

$$\begin{aligned} \sigma &:= \boldsymbol{N}\cdot\boldsymbol{\sigma}\cdot\boldsymbol{N} \\ \sigma_T^2 &:= [\boldsymbol{\sigma}\cdot\boldsymbol{N}]\cdot[\boldsymbol{\sigma}\cdot\boldsymbol{N}\,] - \sigma^2 \end{aligned} \tag{160}$$

Combination of these terms defines the localization ellipse in the Mohr coordinates,

$$\frac{[\sigma-\sigma_o]^2}{A^2} + \frac{\sigma_T^2}{B^2} = 1, \tag{161}$$

where $\sigma_o$ locates the center, while $A$ and $B$ determine the half axes of the ellipse in the normal and tangential stress components, respectively. In the case of the parabolic Drucker-Prager two-invariant model, the normal to the yield surface $\boldsymbol{n}$ and the normal to the plastic potential $\boldsymbol{m}$ take the form.

$$\begin{aligned} \boldsymbol{n} &= \frac{\partial F}{\partial\boldsymbol{\sigma}} = \boldsymbol{s} + \alpha_F\,\mathbf{1} \\ \boldsymbol{m} &= \frac{\partial Q}{\partial\boldsymbol{\sigma}} = \boldsymbol{s} + \alpha_Q\,\mathbf{1} \end{aligned} \tag{162}$$

The abbreviations introduced in Eq.(154) result in the following expressions,

$$\boldsymbol{e}_n = 2\,G\boldsymbol{s}\cdot\boldsymbol{N} + 3\,K\ \alpha_F\ \boldsymbol{N} \tag{163}$$

$$\boldsymbol{e}_m = 2\,G\ \boldsymbol{s}\cdot\boldsymbol{N} + 3\,K\ \alpha_Q\ \boldsymbol{N} \tag{164}$$

The localization ellipse is defined in terms of the parameters

$$\begin{aligned} \sigma_o &= \frac{1}{3}\,I_1 - \frac{1+\nu}{2\,[1-2\nu]}\,[\alpha_F+\alpha_Q] \\ A^2 &= 2\,\frac{1-\nu}{1-2\nu}\,B^2 \\ B^2 &= \frac{1}{4\,G}\,H_p + J_2 + \frac{[1+\nu]^2}{8\,[1-2\nu]\,[1-\nu]}\,[\alpha_F+\alpha_Q]^2 + \frac{1+\nu}{1-\nu}\ \alpha_F\ \alpha_Q \end{aligned} \tag{165}$$

where $\alpha_F, \alpha_Q$ denote the friction and dilatancy parameters of the parabolic Drucker-Prager model.

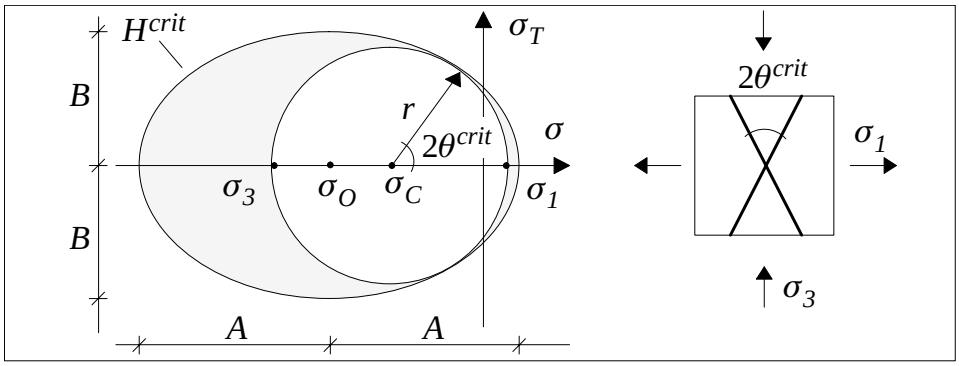


Figure 15: Mohr Representation of Localization Ellipse and Major Stress Circle

The geometrical properties of the localization ellipse is illustrated in Figure 15. Note, that the center and the shape of the ellipse are not influenced by the plastic hardening modulus $H_p$. The hardening modulus only influences the size of the ellipse. Figure 15 depicts also the major Mohr circle of stress,

$$[\sigma - \sigma_c]^2 + \sigma_T^2 = R^2, \tag{166}$$

which characterizes the actual stress state. Herein, $\sigma_c$ and $R$ denote the center and the radius of the circle, respectively in terms of the principal stresses $\sigma_1$ and $\sigma_3$.

$$\begin{aligned} \sigma_c &= \frac{\sigma_1 + \sigma_3}{2} \\ R &= \frac{\sigma_1 - \sigma_3}{2} \end{aligned} \tag{167}$$

The tangency condition results in a quadratic equation, which defines the analytical solutions for critical failure angle $\theta^{crit}$ and the critical hardening modulus $H_p^{loc}$. For the non–associated Drucker–Prager plasticity model, the critical failure angle may be expressed as follows:

$$\tan^2\theta^{crit} = \frac{R - [[1-2\nu]\,[\sigma_c - I_1\,/\,3] + [1+\nu]\,[\alpha_F + \alpha_Q]\,/\,2]}{R + [[1-2\nu]\,[\sigma_c - I_1\,/\,3] + [1+\nu]\,[\alpha_F + \alpha_Q]\,/\,2]} \tag{168}$$

The critical failure angle is strongly influenced by the friction coefficient $\alpha_F$ and the dilatancy parameter $\alpha_Q$. Furthermore, the failure angle is also influenced by Poisson's ratio. The analytical solution for the critical localization modulus takes the following form.

$$\begin{aligned} H_p^{loc} = 4\,G \quad & \left[ [1-2\nu] \left[ \sigma_c - \frac{1}{3} I_1 + \frac{1+\nu}{2\,[1-2\nu]} \,[\alpha_F + \alpha_Q] \right]^2 \right. \\ & \left. + R^2 - J_2 - \frac{[1+\nu]^2}{8\,[1-2\nu]\,[1-\nu]} \,[\alpha_F + \alpha_Q]^2 - \frac{[1+\nu]}{[1-\nu]} \,\alpha_F\,\alpha_Q \right] \end{aligned} \tag{169}$$

which may be positive only in the case of non-associative flow when $\alpha_F \neq \alpha_Q$.

## 4.5 Model Problem of Simple Shear

Under strain control the direct shear experiment exhibits different levels of dilatancy depending on the dyadic product in the plastic portion of the elastoplastic operator assuming that the elastic behavior is isotropic. The confinement of full strain control introduces failure modes that vary from a ductile shear failure mode under high confinement to brittle failure under zero confinement. Thereby, an intriguing consequence of the Reynolds effect is the apparent hardening of the perfectly plastic material model which arises because of the constrained dilatancy.

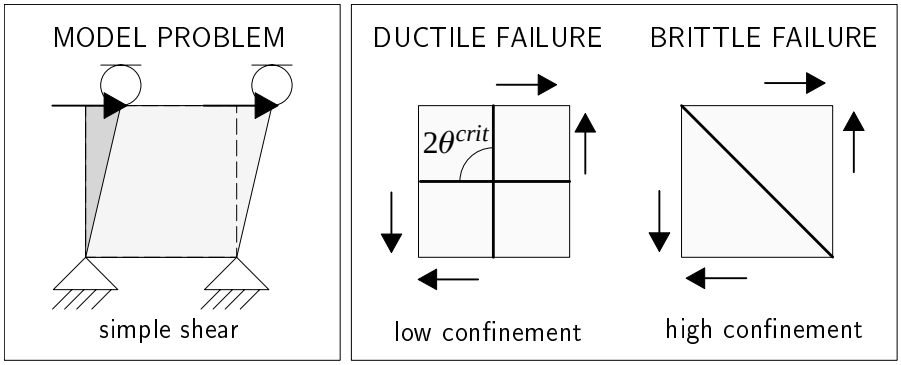


Figure 16: Model Problem – Simple Shear

In the numerical simulation of simple shear the in–plane shear strain $\gamma_{12}$ increases monotonically. The critical directions of localized failure are studied by means of the non–associated parabolic Drucker–Prager plasticity formulation when $\alpha_Q = 0$ which corresponds to incompressible plastic flow. Thereby, the influence of lateral confinement is increased gradually by increasing the contrast ratio of compressive to tensile strength, $f_c' : f_t'$. This ratio directly affects the value of the friction coefficient $\alpha_F$, whereas the parameter $\alpha_Q$ is kept zero according to a plastic potential of the von Mises type.

| $f_c' : f_t'$ | $\nu$=0.000 | $\nu$=0.125 | $\nu$=0.250 | $\nu$=0.375 | $\nu$=0.499 |
|---|---|---|---|---|---|
| 1:1 | $45.00^0$ | $45.00^0$ | $45.00^0$ | $45.00^0$ | $45.00^0$ |
| 3:1 | $35.26^0$ | $33.99^0$ | $32.69^0$ | $31.36^0$ | $30.01^0$ |
| 5:1 | $29.45^0$ | $27.24^0$ | $24.90^0$ | $22.38^0$ | $19.64^0$ |
| 8:1 | $22.20^0$ | $18.26^0$ | $13.37^0$ | $5.39^0$ | $0.00^0$ |
| 12:1 | $11.78^0$ | $0.00^0$ | $0.00^0$ | $0.00^0$ | $0.00^0$ |

Table 1: Critical Failure Angle of Parabolic Drucker-Prager Model – Simple Shear Problem

Table 1 summarizes the critical failure angle $\theta^{crit}$ for different Poisson's ratios and strength ratios $f_c' : f_t'$. The critical failure angles range from $0^0$ to $45^0$, thus including failure modes which range from pure mode I decohesive failure to mode II slip failure. As expected, the critical failure angle decreases with an increase of lateral confinement which is caused by increasing the contrast of the compressive to tensile strength. Moreover, the influence of lateral confinement increases for larger values of Poisson's ratio. Figures 17 to 19 show the result of the corresponding geometric localization analysis for Poisson's ratio

of $\nu = 0.2$. The first figure is for a strength ratio of $f_c' : f_t' = 1 : 1$. This choice corresponds to a vanishing friction coefficient, $\alpha_F = 0.0$, representing the classical yield function of the von Mises type. For this analysis, two critical directions are found under $\theta^{crit} = 45^0$ and $\theta^{crit} = 135^0$ indicating mode II shear failure. This mode is typically observed in pressure-insensitive metals exhibiting Lüders bands.

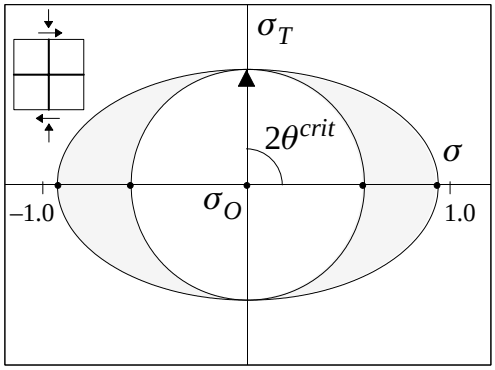


Figure 17: Geometric Localization Analysis – $f_c' : f_t' = 1 : 1$, KUHL & AL [2000].

Figure 18 depicts the result of localization analysis for the strength ratio $f_c' : f_t' = 3 : 1$ representative for cast iron. The corresponding friction coefficient of $\alpha_F = 0.667$ induces relatively low confinement. Again, two critical directions are found, which have rotated slightly towards the direction of maximum principal strain at $45^o$. The corresponding critical failure angles of $\theta = 33.211^0$ and $\theta = 146.79^0$ indicate mixed shear-compression failure.

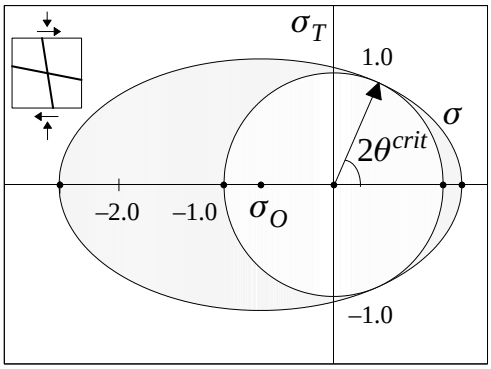


Figure 18: Geometric Localization Analysis – $f_c' : f_t' = 3 : 1$, KUHL & AL [2000].

Finally, the compressive strength is assumed to be twelve times the tensile strength, $f_c' : f_t' = 12 : 1$, which introduces high confinement. The friction coefficient takes a very large value of $\alpha_F = 3.667$, which is representative of cementitious materials like concrete. For this class of materials with a very large contrast between compressive and tensile strength values, a brittle mode of failure is observed. Figure 19 illustrates mode I decohesive failure for which the critical direction corresponds to the direction of maximum principal stress, where $\theta^{crit} = 0^0$.

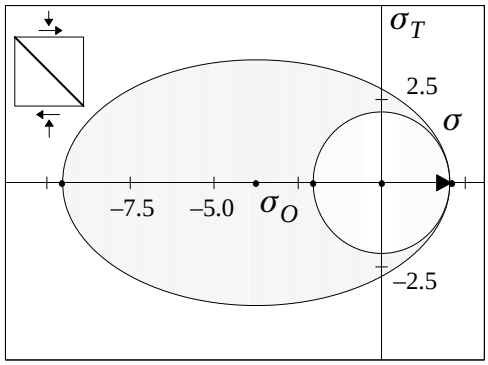


Figure 19: Geometric Localization Analysis – $f_c' : f_t' = 12 : 1$, KUHL & AL [2000].

# 5 Elastic Damage Models

Elastic degradation formulations have received increasing attention since their inception by LAZAR MARKOVICH KACHANOV (1914-1993). Nowadays damage models are used regularly to describe the reduction of the elastic stiffness properties in quasi-brittle materials, such as concrete, rocks, ceramics etc, see LEMAITRE [1992]. For improved realism, additional features have been incorporated beyond the basic format of a scalar damage factor in order to account for different stiffness properties in tension and compression, to capture stiffness recovery due to micro-crack closure, and to model the interaction of damage and plasticity processes.

As indicated in the earlier Section 2.2.1 the basic secant formulation encompasses the simplest format of isotropic damage, which has emerged in the literature. Most scalar damage models start from the basic notion of the effective area concept by Kachanov,

$$A_{eff} = A - A_d = [1-d]A \qquad \text{where} \qquad d = \frac{A_d}{A} \qquad \text{and} \qquad 0 \le d \le 1 \tag{170}$$

according to which the internal stresses are transferred by the intact material skeleton. In other terms, distributed microdefects and stress concentrators reduce the effective load bearing area as compared to the nominal area. This argument leads directly to the effective stress concept through equilibrium considerations, whereby

$$\sigma\, A = \sigma_{eff} A_{eff} \qquad \text{leads to} \qquad \sigma = [1-d]\sigma_{eff} \tag{171}$$

The strain equivalence concept $\epsilon_{eff} = \epsilon$ of a parallel system of damaging elements leads to the classical scalar format of elastic damage,

$$\sigma_{eff} = E\,\epsilon_{eff} \qquad \text{such that} \qquad \sigma = [1-d]E\,\epsilon \tag{172}$$

The $[1-d]$ factor reduces the elastic stiffness properties, when $d = 0 \to 1$. In summary, the elementary damage model leads to the secant stress-strain relationship,

$$\sigma = E_s\,\epsilon \qquad \text{where} \qquad E_s = [1-d]E \qquad \text{and} \qquad d = 1 - \frac{E_s}{E} \tag{173}$$

For a more differentiated isotropic approach the degradation distinguishes between volumetric and deviatoric damage. In the case of anisotropic degradation a number of representations have been proposed, starting from vector, to second, fourth and eight order tensor formulations. Thereby, the most popular concept is the second order damage tensor $[d_{ij}] = \boldsymbol{d}$ and its equivalent integrity tensor,

$$\boldsymbol{\phi} = \mathbf{1} - \boldsymbol{d} \quad \text{or} \quad \phi_{ij} = \delta_{ij} - d_{ij} \tag{174}$$

Whereas the secant formulation of elastic stiffness degradation is well established for isotropic as well as anisotropic damage, the constitutive formulation of the damage process requires a loading function, a damage rule and some hardening softening laws that describe the degradation process in terms of a reduced number of internal variables. In the spirit of the internal variable theory they need to be defined in the space of conjugate thermodynamic forces, which turns out to be the strain energy density function when a scalar damage variable is used.

## 5.1 Basic Format of Elastic Scalar Damage

In the traditional $[1-d]$ model of scalar damage, the isotropic stiffness and compliance tensors are replaced by their secant values,

$$\boldsymbol{\mathcal{E}}_s = [1-d]\boldsymbol{\mathcal{E}}_o \quad \text{and} \quad \boldsymbol{\mathcal{C}}_s = \frac{1}{1-d}\boldsymbol{\mathcal{C}}_o \tag{175}$$

Differentiation of the secant relations leads to,

$$\dot{\boldsymbol{\mathcal{E}}}_s = -\dot{d}\boldsymbol{\mathcal{E}}_o \quad \text{and} \quad \dot{\boldsymbol{\mathcal{C}}}_s = \frac{\dot{d}}{1-d}\boldsymbol{\mathcal{C}}_s \tag{176}$$

The compliance term suggests to change variables and to use the logarithmic scalar damage variable,

$$\dot{\ell} = \frac{\dot{d}}{1-d} \quad \text{where} \quad \ell = \int \dot{\ell} = ln(\frac{1}{1-d}) \quad \text{and} \quad d = 1 - e^{-\ell} \tag{177}$$

This permits us to rewrite the secant tensors and the derivative of the compliance in the form of

$$\boldsymbol{\mathcal{E}}_s = e^{-\ell}\boldsymbol{\mathcal{E}}_o \quad \text{and} \quad \boldsymbol{\mathcal{C}}_s = e^{\ell}\,\boldsymbol{\mathcal{C}}_o \quad \text{such that} \quad \dot{\boldsymbol{\mathcal{C}}}_s = \dot{\ell}\,\boldsymbol{\mathcal{C}}_s \tag{178}$$

In analogy to plastic associativity we need to examine the thermodynamic force conjugate to the damage variable in the dissipation inequality. The recoverable part of the elastic energy density is a function of the current secant stiffness or compliance properties, i.e.

$$2W = \boldsymbol{\epsilon} : \boldsymbol{\mathcal{E}}_s : \boldsymbol{\epsilon} = \boldsymbol{\sigma} : \boldsymbol{\mathcal{C}}_s : \boldsymbol{\sigma} \tag{179}$$

Differentiation leads to the following energy exchange

$$\dot{W} = \boldsymbol{\sigma} : \dot{\boldsymbol{\epsilon}} - \frac{1}{2}\boldsymbol{\sigma} : \dot{\boldsymbol{\mathcal{C}}}_s : \boldsymbol{\sigma} \tag{180}$$

where $\boldsymbol{\sigma} : \dot{\boldsymbol{\epsilon}}$ is the external energy supply and $\dot{W}$ the increase of elastic strain energy density. Thus, the difference defines the dissipation rate, which must remain positive according to the second thermodynamic law,

$$\dot{\mathcal{D}} = \boldsymbol{\sigma} : \dot{\boldsymbol{\epsilon}} - \dot{W} = \frac{1}{2}\boldsymbol{\sigma} : \dot{\boldsymbol{\mathcal{C}}}_s : \boldsymbol{\sigma} \geq 0 \tag{181}$$

The thermodynamic force $\boldsymbol{\mathcal{Y}}$, which is taken to be conjugate to the basic change of the secant compliance, is

$$\dot{\mathcal{D}} = -\boldsymbol{\mathcal{Y}} :: \dot{\boldsymbol{\mathcal{C}}}_s \quad \text{where} \quad -\boldsymbol{\mathcal{Y}} = \frac{1}{2}\boldsymbol{\sigma} \otimes \boldsymbol{\sigma} \tag{182}$$

In the scalar format of logarithmic damage, the thermodynamic conjugate force reduces to the elastic strain energy density function $W$, as

$$\dot{\mathcal{D}} = -\boldsymbol{\mathcal{Y}} :: \boldsymbol{\mathcal{C}}_s \dot{\ell} = \frac{1}{2}\boldsymbol{\sigma} : \boldsymbol{\mathcal{C}}_s : \boldsymbol{\sigma} \dot{\ell} = W \dot{\ell} \tag{183}$$

For associativity, the damage function needs to be expressed in terms of the conjugate thermodynamic force, which delimits the undamaged response regime of the strain energy resistance function $r_d$ in analogy to the yield condition of plasticity,

$$F_d = F(W, \ell) = W - r_d(\ell) = 0 \tag{184}$$

In other terms, the resistance function $r_d = W$ is the internal strain energy of a specific test environment following the classical argument of Beltrami, or its deviatoric component in the case of the distortional energy criterion of Huber.

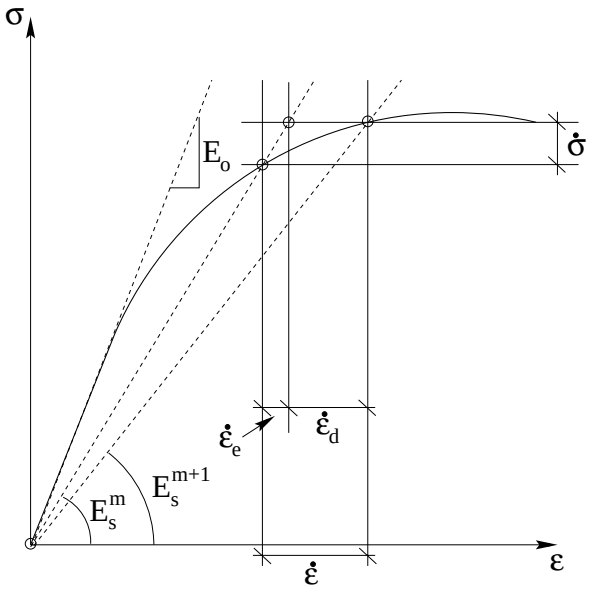


Figure 20: Response Behavior of Elastic Degradation

The derivation follows the elastoplastic format developed by Carol, Rizzi & Willam [2001] for elastic dagradation. Starting from the decomposition of strain rate into an elastic stress producing and

a degrading strain component, $\dot{\boldsymbol{\epsilon}} = \dot{\boldsymbol{\epsilon}}_e + \dot{\boldsymbol{\epsilon}}_d$, illustrated in Figure 20, the current secant stiffness is being used to differentiate between the elastic stress producing deformations and the inelastic damage stress. This results in zero permanent deformations under load-unload cycles, though dissipation will take place according to the degree of nonlinearity during loading as opposed to linear unloading.

The set of rate equations which describes progressive degradation follows the individual steps of the flow theory of plasticity:

1. *Stress-Strain Rate Relation:* $\boldsymbol{\sigma} = \boldsymbol{\mathcal{E}}_s : \boldsymbol{\epsilon}$ and $\dot{\boldsymbol{\sigma}} = \boldsymbol{\mathcal{E}}_s : [\dot{\boldsymbol{\epsilon}} - \dot{\boldsymbol{\epsilon}}_d]$
   where the rate of damage strain defines the deviation from linearity with regard to the linear secant stiffness as indicated n Figure 20.

2. *Damage Rule:* $\dot{\boldsymbol{\epsilon}}_d = \dot{\lambda}\boldsymbol{m}_d$,
   where $\boldsymbol{m}_d = \boldsymbol{\mathcal{C}}_s : \boldsymbol{\sigma} = \boldsymbol{\epsilon}$ defines the directional properties of elastic degradation, and where the damage multiplier $\dot{\lambda}$ defines the magnitude of the inelastic damage strain.

3. *Damage Threshold Condition:* $F_d = f(\boldsymbol{\mathcal{Y}}) - r_d(\lambda) = 0$,
   where $f(\boldsymbol{\mathcal{Y}})$ denotes the demand in terms of a scalar-valued representation of the conjugate force in the dissipation inequality, and where $r_d$ defines the threshold resistance function.

4. *Consistency Condition for Persistent Elastic Damage:* $\dot{F}_d = \boldsymbol{n}_d : \dot{\boldsymbol{\sigma}} - H_d\dot{\lambda} = 0$,
   where $\boldsymbol{n}_d = \frac{\partial F_d}{\partial \boldsymbol{\sigma}}$ is the gradient of the damage function and where $H_d = -\frac{\partial F_d}{\partial \lambda}$ denotes the hardening/softening modulus of the resistance function.

5. *Damage Multiplier:* $\dot{\lambda} = \frac{1}{h_d}\boldsymbol{n} : \boldsymbol{\mathcal{E}}_s : \dot{\boldsymbol{\epsilon}}$
   where the strain-driven format of damage introduces the denominator $h_d = H_d + \boldsymbol{n}_d : \boldsymbol{\mathcal{E}}_s : \boldsymbol{m}_d$ which is subject to the same constraint, $h_d > 0$, as the analogous denominator term in elastoplasticity. This leads to the critical softening modulus for elastic damage $H_d^{crit} = -\boldsymbol{n}_d : \boldsymbol{\mathcal{E}}_s : \boldsymbol{m}_d$.

6. *Tangential Scalar Damage Properties:* $\boldsymbol{\mathcal{E}}_{ed} = \boldsymbol{\mathcal{E}}_s - \frac{1}{h_d}\boldsymbol{\mathcal{E}}_s : \boldsymbol{m}_d \otimes \boldsymbol{n}_d : \boldsymbol{\mathcal{E}}_s$
   where the main difference from elastoplasticity is the secant reference stiffness. The constitutive format has the same structure as elastoplasticity except that $\boldsymbol{\mathcal{E}}_s \neq const.$.

In the isotropic case of the logarithmic scalar damage model, $\dot{\lambda} = \dot{\ell}$, and both, the damage rule as well as the gradient of the damage function are associative as long as the damage function is expressed in terms of the conjugate force,

$$F_d = W - r_d(\ell) = 0 \quad \text{with} \quad \boldsymbol{n}_d = \frac{\partial F_d}{\partial \boldsymbol{\sigma}} = \boldsymbol{\mathcal{C}}_s : \boldsymbol{\sigma} = \boldsymbol{\epsilon} \tag{185}$$

The hardening/softening modulus $H_d$ at constant stress is defined as,

$$H_d = -\frac{\partial F_d}{\partial \lambda} = \frac{\partial r_d}{\partial \ell} \tag{186}$$

From these terms the tangent stiffness of elastic degradation may be assembled in the standard manner which yields,

$$\boldsymbol{\mathcal{E}}_{ed} = e^{-\ell}\boldsymbol{\mathcal{E}}_s - \frac{1}{h_d}\boldsymbol{\sigma}\otimes\boldsymbol{\sigma} \tag{187}$$

where the denominator $h_d = \frac{\partial r_d}{\partial \ell} + \boldsymbol{\sigma} : \boldsymbol{\epsilon}$ must remain strictly positive under strain control. The symmetric format of the tangent stiffness operator is a consequence of the associative damage function, in contrast to damage functions such as the strain-based damage model of Mazars and his co-workers.

## 5.2 Simple Shear Response of Logarithmic Scalar Damage Model

In what follows we compare the results of the scalar-valued damage formulation with the corresponding elastoplastic results in Section 3.4 in order to assess their volumetric-deviatoric interaction.

In analogy to plasticity, the elastic damage matrix may be partitioned into four submatrices which correspond to the normal and shear components of stress and strain. In the case of isotropic elasticity, there is no coupling between elastic normal and shear stresses, and normal and shear strains in the initial stage before damage takes place.

Strain control of the simple shear test results in $\tau_{12} = G_0\gamma_{12}$ at the onset of damage. Substituting into the elastic damage operator leads to the rate equations

$$\begin{Bmatrix} \dot\sigma_{11} \\ \dot\sigma_{22} \\ \dot\sigma_{33} \\ \cdots \\ \dot\tau_{12} \\ \dot\tau_{23} \\ \dot\tau_{13} \end{Bmatrix} = e^{-\ell} \left[\begin{array}{ccc:ccc} K_o+\frac{4}{3}G_o & K_o-\frac{2}{3}G_o & K_o-\frac{2}{3}G_o & 0 & 0 & 0 \\ K_o-\frac{2}{3}G_o & K_o+\frac{4}{3}G_o & K_o-\frac{2}{3}G_o & 0 & 0 & 0 \\ K_o-\frac{2}{3}G_o & K_o-\frac{2}{3}G_o & K_o+\frac{4}{3}G_o & 0 & 0 & 0 \\ \hdashline 0 & 0 & 0 & G_o-\frac{e^\ell}{h_d}\tau_{12}^2 & 0 & 0 \\ 0 & 0 & 0 & 0 & G_o & 0 \\ 0 & 0 & 0 & 0 & 0 & G_o \end{array}\right] \begin{Bmatrix} 0 \\ 0 \\ 0 \\ \cdots \\ \dot\gamma_{12} \\ 0 \\ 0 \end{Bmatrix} \tag{188}$$

The coupling partitions are zero showing no interaction between the normal stresses and the shear strains, when the material experiences damage in analogy to the relation in Eq.(106) for $J_2$-plasticity.

### 5.2.1 Singularity of Tangent Damage Operator

Possible singularities of $\boldsymbol{E}_{ed}$ may be studied again with the Schur theorem of zero sub-determinant. We note that the normal partition of the stiffness matrix $\boldsymbol{E}^{ed}_{nn}$ simply reflects the degradation of the intact elastic partition $\boldsymbol{E}^{0}_{nn}$ by the integrity factor $e^{-\ell} = 1 - d$ as $\ell \to \infty$. The second possibility, which could cause the tangent operator to become singular, is the shear partition, $\boldsymbol{E}^{ed}_{ss}$. The two diagonal terms $E^{ed}_{55}$ and $E^{ed}_{66}$ are affected by degradation of the elastic properties, they will induce a singularity only when $e^{-\ell} \to 0$. The diagonal term $E^{ed}_{44}$ however, can diminish to zero before the material is fully damaged, since

$$E^{ed}_{44} = e^{-\ell}G_o - \frac{1}{h_d}\tau_{12}^2 = 0 \tag{189}$$

when

$$h_d = \frac{\tau_{12}^2}{e^{-\ell}G_o} = \frac{\tau_{12}^2}{G_s} = \tau_{12}\gamma_{12} \tag{190}$$

The damage denominator $h_d = H_d + \boldsymbol{\sigma} : \boldsymbol{\epsilon}$ infers that the hardening modulus must be zero, i.e.

$$H_d = \frac{\partial r}{\partial \ell} = 0 \quad \text{when} \quad h_d = \tau_{12}\gamma_{12} \tag{191}$$

for any value of damage, $\ell$. Thus for perfectly damaging behavior, when $H_d = 0$ we have $E^{ed}_{44} = 0$, and consequently the tangent operator turns singular, $\det \boldsymbol{E}_{ed} = 0$. This behavior is very much analogous to pressure-insensitive von Mises plasticity and holds independently of the load condition, when elastic damage is restricted to the deviatoric response behavior.

## 5.3 Damage Models under Simple Shear

To illustrate the performance of damage models let us consider again the strain-controlled load case of simple shear. To start with, we examine the relationship between scalar damage mechanics and the earlier development of one-invariant von Mises plasticity. Comparing the governing tangent operators in Eqs.(88) and (188) we recognize the same structure except for the integrity factor $e^{-\ell}$ in the case of scalar damage. Using the equivalent energy density value to calibrate the damage threshold $r_d = \frac{1}{2G}\tau_y^2$, Figure 21a shows that the response behavior is identical to that of elastoplasticity shown for monotonic loading in Figure 8a. The basic difference between damage and plasticity shows up when we consider cyclic loading which takes place along the degraded secant stiffness, and which does not distinguish between tension and compression because of the underlying Beltrami condition of a maximum strain energy threshold. There is no confinement effect and the shear strength in this strain-controlled problem coincides with the tensile strength. Since the simple shear response may be viewed as an equi-biaxial tension-compression test with no direct-shear coupling, all damage stresses degrade exponentially according to the logarithmic damage evolution, in tension as well as in compression and shear.

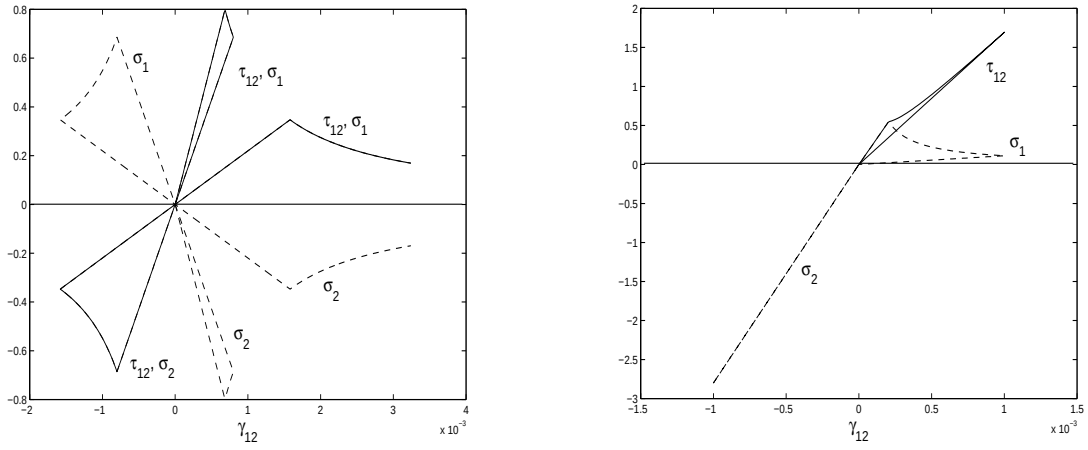


Figure 21: Simple Shear Response: (a) Scalar Damage Model, (b) Anisotropic Damage Model, CAROL ET AL [2001].

In contrast, we consider the recent anisotropic damage formulation of CAROL, RIZZI & WILLAM [2001] to examine the influence of anisotropy on the volumetric-deviatoric interaction. In this case a second order integrity tensor $\boldsymbol{\phi} = \mathbf{1} - \boldsymbol{d}$ is adopted in extension of the pseudo-logarithmic scalar format

above. Resorting to the so-called energy equivalence of Cordebois & Sidoroff, where neither effective stress nor effective strain coincides with their nominal counterparts, we develop a fourth order damage effect tensor,

$$\boldsymbol{\sigma}_{eff} = \boldsymbol{\alpha} : \boldsymbol{\sigma} \qquad \text{and} \qquad \boldsymbol{\epsilon} = \boldsymbol{\alpha}^t : \boldsymbol{\epsilon}_{eff} \tag{192}$$

Assuming linear elastic behavior at the level of effective stress and effective strain, the resulting secant compliance retains symmetry,

$$\boldsymbol{\mathcal{C}}_s = \boldsymbol{\alpha}^t : \boldsymbol{\mathcal{C}} : \boldsymbol{\alpha} \tag{193}$$

In the principal axes of damage, the damage effect tensor reduces to diagonal form,

$$\boldsymbol{\alpha} = \left[\begin{array}{ccc|ccc} \phi_1 & 0 & 0 & & & \\ 0 & \phi_2 & 0 & & 0 & \\ 0 & 0 & \phi_3 & & & \\ \hline & & & \sqrt{\phi_1\phi_2} & & \\ & 0 & & & \sqrt{\phi_2\phi_3} & \\ & & & & & \sqrt{\phi_3\phi_1} \end{array}\right] \tag{194}$$

Consequently, the corresponding secant compliance of anisotropic damage has the format,

$$\boldsymbol{C}_s = \frac{1}{E}\left[\begin{array}{ccc|ccc} \phi_1^2 & -\nu\phi_1\phi_2 & -\nu\phi_1\phi_3 & & & \\ -\nu\phi_2\phi_1 & \phi_2^2 & -\nu\phi_2\phi_3 & & 0 & \\ -\nu\phi_3\phi_1 & -\nu\phi_3\phi_2 & \phi_3^2 & & & \\ \hline & & & 2[1+\nu]\phi_1\phi_2 & & \\ & 0 & & & 2[1+\nu]\phi_2\phi_3 & \\ & & & & & 2[1+\nu]\phi_3\phi_1 \end{array}\right] \tag{195}$$

where the secant stiffness involves five independent material parameters as opposed to nine in orthotropic elasticity. For damage evolution we need to define a damage criterion. For associated damage the demand function $F_d = f(\boldsymbol{\mathcal{Y}}) - r_d(\ell) = 0$ is based on the conjugate force which is in this case the second order energy tensor $\boldsymbol{\mathcal{Y}} = \boldsymbol{\sigma} \cdot \boldsymbol{\epsilon}$. In this case, we resort to the Rankine criterion of maximum 'principal energy' where the scalar damage function is $F_d = \mathcal{Y}_{max} - r_d(\ell) = 0$. Adopting a no damage switch in compression, the simple shear response results in the response behavior shown in Figure 21b. In comparison to the scalar damage format in Figure 21a, the simple shear response of the anisotropic damage model in Figure 21b shows some very interesting features: (i) after reaching the damage threshold at $\tau_{12} = 0.8\, ksi$, the principal tensile stress diminishes again exponentially, (ii) the shear stress and the compressive principal stress increase without bounds because of volumetric-deviatoric interaction which introduces increasing confinement. Moreover, there is no damage in compression, and unloading occurs at the secant stiffness in tension leaving no permanent deformation, while the compressive stiffness remains intact.

In contrast to the scalar damage model, we notice that the anisotropic damage model does exhibit volumetric-deviatoric coupling. Thereby, the shear stress increases far beyond the initial shear strength threshold $\tau_y = 0.8\, ksi$ in the presence of out-of-plane confinement. At the same time, the nominal tensile

stress is subject to softening due to progressive tensile damage according to the logarithmic degradation law.

In summary, isotropic scalar damage models do not exhibit shear dilatancy, while anisotropic models do reproduce the Reynolds dilatancy effect of frictional materials similarly to pressure-sensitive plasticity.

# 6 Conclusions

The present state-of-the art report focused on major developments in rate independent elasticity and inelasticty. Many topics have not been covered for the sake of brevity, most notably are nonlinear hardening and softening formats in plasticity and damage, LUBLINER [1990], the general form of the internal variable description,HALPHEN & NGUYEN [1975], the microstructural features thereof, KRÖNER [1963], the size and gradient effects, BAŽANT & PLANAS [1997], and last but not least, the computational aspects of inelastic analysis.

The exposition presented an apercu of linear and nonlinear elastic constitutive models as well as plastic and elastic damage models. Specifically we have examined the interaction of normal and shear components which is directly related to the population in the constitutive gradients $\boldsymbol{n}, \boldsymbol{m}$ responsible for stress- and/or strain-induced anisotropy in the tangent operator.

# 7 Acknowledgements

The author wishes to acknowledge the help of Dr. Eric Hansen and former co-workers Dr. Ellen Kuhl and Dr. Hong Kang for their assistance and for preparing some of the figures. The state-of-the art report was partially sponsored by the National Science Foundation grant CMS 9634923 to the University of Colorado Boulder. Opinions expressed in this paper are those of the writer and do not reflect those of the sponsor.

# References

[1] BAŽANT, Z. P. & J. PLANAS [1997]. *Fracture and Size Effect in Concrete and Other Quasibrittle Materials.* CRC Press, Boca Raton, Florida.

[2] BENALLAL, A. & C. COMI [1996]. 'Localization analysis via a geometrical method.' *Int. J. Solids & Structures*, **33**, pp. 99–119.

[3] CAROL, I., RIZZI, E. AND WILLAM, K. [2001]. 'On the formulation of anisotropic elastic degradation. Part I: Theory based on a pseudo-logarithmic damage tensor rate, and Part II: Generalized pseudo-Rankine model for tensile damage.' *Int. J. Solids & Structures*, **38**, pp. 491–546.

[4] CHEN, W.F. AND D.J. HAN [1988]. *Plasticity for Structural Engineers.* Springer Verlag, New York.

[5] COLEMAN, B.D. & M.E. GURTIN [1967]. 'Thermodynamics with internal state variables.' *J. of Chemical Physics*, **47**, pp. 597–613.

[6] Drucker, D. C. & W. Prager [1952]. 'Soil mechanics and plastic analysis of limit design.' *Quarterly Appl. Math.*, **10**, pp. 157–175.

[7] Halphen, B. & Q.S. Nguyen [1975]. 'Sur les matériaux standards généralisés'. *J. de Mécanique*, **14/1**, pp. 39–63.

[8] Kang, H. & K. Willam [1999]. 'Localization characteristics of a triaxial concrete model.' *ASCE J. Eng. Mech.*, **125**, pp. 941–950.

[9] Kröner, E. [1963]. Dislocation: a new concept in the continuum thery of platicity. *J. Math. & Phys.*, **42**, pp. 27-37.

[10] Kuhl, E., Ramm, E. & K. Willam [2000]. 'Failure analysis of elasto-plastic materials at different levels of observation.' *Intl. J. Solids and Structures*, **37**, 48-50, pp. 7259-7280.

[11] Lemaitre, J., [1992]. *A Course on Damage Mechanics*. Springer-Verlag Berlin, Germany.

[12] Lubliner, J., [1990]. *Plasticity Theory*. Macmillan Publishing Company, New York.

[13] Maier, G. & T. Hueckel [1979]. 'Nonassociated and coupled flow rules of elastoplasticity for rock-like materials'. *Int. J. Rock Mech.& Min. Sci.*, **16**, pp. 77–92.

[14] Ogden, R.W. [1984]. *Non-Linear Elastic Deformations*. Ellis Horwood Limited Publ., Chichester, UK.

[15] Ottosen, N. S. & K. Runesson [1991]. 'Properties of discontinuous bifurcation solutions in elasto-plasticity.' *Int. J. Solids & Structues*, **27**, pp. 401–421.

[16] Rudnicki, J. W. & J. R. Rice [1975]. 'Conditions for the localization of deformation in pressure-sensitive dilatant materials.' *J. Mech. Phys. Solids*, **23**, pp. 371–394.

[17] Valanis, K.C. [1975]. 'On the foundations of the endochronic theory of viscoplasticity'. *Arch. Mech. Stos.*, **27**, pp. 857–868.

[18] Willam, K. J. & E.P. Warnke [1975]. 'Constitutive Model for the Triaxial Behaviour of Concrete'. *Proc. Intl. Assoc. Bridge Structl. Engrs*, Report 19, Section III, Zürich, Switzerland, pp. 1–30.

# 8 Appendix I: Some Results of Matrix and Tensor Analysis

The mathematical tools behind material models are housed in linear algebra and tensor analysis in particular. For this reason we revisit a few well-established relationships, which hopefully provide additional insight beyond the mere mechanics of elementary matrix and tensor manipulation.

## 8.1 Voigt Notation

In this review Voigt notation is used to compact symmetric stress and strain tensors and their interrelationship. Here we briefly summarize results of inner and dyadic products which have important consequences when anisotropic stiffness and compliance relations are considered. For the sake of argument we compare the matrix notation of non-symmetric stress and strain tensors with the corresponding reduced matrix notation of Voigt which is based on the technical definition of shear strain.

For simplicity we consider the state of plane stress and strain and express the second order tensors in terms of Cartesian coordinates

$$\boldsymbol{\sigma} = \begin{bmatrix} \sigma_{11} & \sigma_{12} \\ \sigma_{21} & \sigma_{22} \end{bmatrix}; \quad \boldsymbol{\epsilon} = \begin{bmatrix} \epsilon_{11} & \epsilon_{12} \\ \epsilon_{21} & \epsilon_{22} \end{bmatrix} \tag{196}$$

In vector notation the stress and strain tensors write as,

$$\boldsymbol{\sigma}_{tens} = \begin{bmatrix} \sigma_{11} & \sigma_{22} & \sigma_{12} & \sigma_{21} \end{bmatrix}^t; \quad \boldsymbol{\epsilon}_{tens} = \begin{bmatrix} \epsilon_{11} & \epsilon_{22} & \epsilon_{12} & \epsilon_{21} \end{bmatrix}^t \tag{197}$$

Consequently, the scalar product of the internal energy $2W = \boldsymbol{\sigma} : \boldsymbol{\epsilon}$ is in vector notation,

$$2W = \boldsymbol{\sigma}^t_{tens}\boldsymbol{\epsilon}_{tens} = \sigma_{11}\epsilon_{11} + \sigma_{22}\epsilon_{22} + \sigma_{21}\epsilon_{21} + \sigma_{12}\epsilon_{12} \tag{198}$$

The corresponding dyadic product $\boldsymbol{\sigma} \otimes \boldsymbol{\epsilon}$ results in the matrix representation of the fourth order tensor,

$$\boldsymbol{\sigma}_{tens}\boldsymbol{\epsilon}^t_{tens} = \begin{bmatrix} \sigma_{11}\epsilon_{11} & \sigma_{11}\epsilon_{22} & \sigma_{11}\epsilon_{12} & \sigma_{11}\epsilon_{21} \\ \sigma_{22}\epsilon_{11} & \sigma_{22}\epsilon_{22} & \sigma_{22}\epsilon_{12} & \sigma_{22}\epsilon_{21} \\ \sigma_{12}\epsilon_{11} & \sigma_{12}\epsilon_{22} & \sigma_{12}\epsilon_{12} & \sigma_{12}\epsilon_{21} \\ \sigma_{21}\epsilon_{11} & \sigma_{21}\epsilon_{22} & \sigma_{21}\epsilon_{12} & \sigma_{21}\epsilon_{21} \end{bmatrix} \tag{199}$$

Linear elasticity $\boldsymbol{\sigma} = \boldsymbol{\mathcal{E}} : \boldsymbol{\epsilon}$ exhibits general anisotropy in matrix notation,

$$\begin{Bmatrix} \sigma_{11} \\ \sigma_{22} \\ \cdots \\ \sigma_{12} \\ \sigma_{21} \end{Bmatrix} = \begin{bmatrix} E_{1111} & E_{1122} & \vdots & E_{1112} & E_{1121} \\ E_{2211} & E_{2222} & \vdots & E_{2212} & E_{2221} \\ \cdots & \cdots & \cdots & \cdots & \cdots \\ E_{1211} & E_{1222} & \vdots & E_{1212} & E_{1221} \\ E_{2111} & E_{2122} & \vdots & E_{2112} & E_{2121} \end{bmatrix} \begin{Bmatrix} \epsilon_{11} \\ \epsilon_{22} \\ \cdots \\ \epsilon_{12} \\ \epsilon_{21} \end{Bmatrix} \tag{200}$$

where the elastic stiffness matrix involves ten in-plane elastic moduli in the case of material symmetry when $\boldsymbol{\mathcal{E}} = \boldsymbol{\mathcal{E}}^t$. The anisotropy reduces to six moduli in the case of symmetric stress and strain tensors, when $\boldsymbol{\sigma} = \boldsymbol{\sigma}^t$ and $\boldsymbol{\epsilon} = \boldsymbol{\epsilon}^t$.

Restricting the exposition to symmetric stress and strain tensors, Voigt notation takes advantage the reduced dimension from four to three components in the case of plane stress.

$$\boldsymbol{\sigma}_{voigt} = \begin{bmatrix} \sigma_{11} & \sigma_{22} & \tau_{12} \end{bmatrix}^t; \quad \boldsymbol{\epsilon}_{voigt} = \begin{bmatrix} \epsilon_{11} & \epsilon_{22} & \gamma_{12} \end{bmatrix}^t \tag{201}$$

where $\tau_{ij} = \sigma_{ij}$, $\gamma_{ij} = 2\epsilon_{ij}, \forall i \neq j$.

The scalar product of internal energy $2W = \boldsymbol{\sigma} : \boldsymbol{\epsilon}$ writes in Voigt notation,

$$2W = \boldsymbol{\sigma}^t_{voigt} \boldsymbol{\epsilon}_{voigt} = \sigma_{11}\epsilon_{11} + \sigma_{22}\epsilon_{22} + \tau_{21}\gamma_{21} \tag{202}$$

Reducing the dimension of the strain tensor corresponds to the kinematic constraint $\boldsymbol{\epsilon}_{tens} = \boldsymbol{T}\, \boldsymbol{\epsilon}_{voigt}$ which takes advantage of symmetric shear strains,

$$\left\{ \begin{array}{c} \epsilon_{11} \\ \epsilon_{22} \\ \epsilon_{12} \\ \epsilon_{21} \end{array} \right\} = \left[ \begin{array}{ccc} 1 & 0 & 0 \\ 0 & 1 & 0 \\ 0 & 0 & 0.5 \\ 0 & 0 & 0.5 \end{array} \right] \left\{ \begin{array}{c} \epsilon_{11} \\ \epsilon_{22} \\ \gamma_{12} \end{array} \right\} \tag{203}$$

Using the principle of virtual work to preserve the energy of the unreduced format, the conjugate transformation of the symmetrized stress and strain follows as,

$$\delta\boldsymbol{\epsilon}^t_{tens}\boldsymbol{\sigma}_{tens} = \delta\boldsymbol{\epsilon}^t_{voigt}\boldsymbol{\sigma}_{voigt}; \quad \text{and thus} \quad \delta\boldsymbol{\epsilon}^t_{voigt}\boldsymbol{T}^t\boldsymbol{\sigma}_{tens} = \delta\boldsymbol{\epsilon}^t_{voigt}\boldsymbol{\sigma}_{voigt} \tag{204}$$

In other terms, the reduction of the stress tensor follow the transposed transformation, $\sigma_{voigt} = \boldsymbol{T}^t\boldsymbol{\sigma}_{tens}$.

$$\left\{ \begin{array}{c} \sigma_{11} \\ \sigma_{22} \\ \tau_{12} \end{array} \right\} = \left[ \begin{array}{cccc} 1 & 0 & 0 & 0 \\ 0 & 1 & 0 & 0 \\ 0 & 0 & 0.5 & 0.5 \end{array} \right] \left\{ \begin{array}{c} \sigma_{11} \\ \sigma_{22} \\ \sigma_{12} \\ \sigma_{21} \end{array} \right\} \tag{205}$$

Consequently the scalar energy product leads to the compact format,

$$2W = \boldsymbol{\sigma}^t_{tens}\boldsymbol{\epsilon}_{tens} = \boldsymbol{\sigma}^t_{voigt}\boldsymbol{T}^{-1}\boldsymbol{T}\boldsymbol{\epsilon}_{voigt} = \boldsymbol{\sigma}^t_{voigt}\boldsymbol{\epsilon}_{voigt} \tag{206}$$

The linear elastic material relation $\boldsymbol{\sigma} = \boldsymbol{\mathcal{E}} : \boldsymbol{\epsilon}$ compacts in Voigt notation into

$$\boldsymbol{\sigma}_{tens} = \boldsymbol{E}_{tens}\boldsymbol{\epsilon}_{tens}; \quad \text{or} \quad \boldsymbol{\sigma}_{voigt} = \boldsymbol{E}_{voigt}\boldsymbol{\epsilon}_{voigt} \tag{207}$$

where

$$\boldsymbol{E}_{voigt} = \boldsymbol{T}^t\boldsymbol{E}_{tens}\boldsymbol{T} \tag{208}$$

In other terms the $4 \times 4$ elasticity matrix reduces to the traditional $3 \times 3$ format of $\boldsymbol{E}_{voigt} = \boldsymbol{E}$ commonly used in engineering notation with six moduli of anisotropy in planar elasticity.

$$\left\{ \begin{array}{c} \sigma_{11} \\ \sigma_{22} \\ \cdots \\ \tau_{12} \end{array} \right\} = \left[ \begin{array}{ccc} E_{1111} & E_{1122} & \vdots \quad 0.5[E_{1112} + E_{1121}] \\ E_{2211} & E_{2222} & \vdots \quad 0.5[E_{2212} + E_{2221}] \\ \cdots\cdots & \cdots\cdots & \cdots\cdots\cdots\cdots \\ 0.5[E_{1211} + E_{2111}] & 0.5[E_{1222} + E_{2122}] & \vdots \quad 0.25[E_{1212} + E_{1221} + E_{2112} + E_{2121}] \end{array} \right] \left\{ \begin{array}{c} \epsilon_{11} \\ \epsilon_{22} \\ \cdots \\ \gamma_{12} \end{array} \right\} \tag{209}$$

In engineering notation we normally refer to the elasticity matrix which for isotropic plane strain conditions reduces to the traditional format,

$$\boldsymbol{E}_{voigt} = \begin{bmatrix} E_{11} & E_{12} & \vdots & E_{13} \\ E_{21} & E_{22} & \vdots & E_{23} \\ \cdots & \cdots & \cdots & \cdots \\ E_{31} & E_{32} & \vdots & E_{33} \end{bmatrix} \rightarrow \begin{bmatrix} \Lambda + 2G & \Lambda & \vdots & 0 \\ \Lambda & \Lambda + 2G & \vdots & 0 \\ \cdots & \cdots & \cdots & \cdots \\ 0 & 0 & \vdots & G \end{bmatrix} \tag{210}$$

To amplify the reduction process we consider the case of stress-induced anisotropy in plasticity where the dyadic product involves the gradient of the plastic potential and the yield function, $\boldsymbol{m} \otimes \boldsymbol{n}$. Tensor notation of the unreduced $4 \times 4$ system reads

$$\boldsymbol{m}_{tens}\boldsymbol{n}^t_{tens} = \begin{bmatrix} m_{11}n_{11} & m_{11}n_{22} & m_{11}n_{12} & m_{11}n_{21} \\ m_{22}n_{11} & m_{22}n_{22} & m_{22}n_{12} & m_{22}n_{21} \\ m_{12}n_{11} & m_{12}n_{22} & m_{12}n_{12} & m_{12}n_{21} \\ m_{21}n_{11} & m_{21}n_{22} & m_{21}n_{12} & m_{21}n_{21} \end{bmatrix} \tag{211}$$

Reduction to Voigt notation,

$$\boldsymbol{m}_{voigt}\boldsymbol{n}^t_{voigt} = \begin{bmatrix} m_{11}n_{11} & m_{11}n_{22} & 0.5[m_{11}n_{12} + m_{11}n_{21}] \\ m_{22}n_{11} & m_{22}n_{22} & 0.5[m_{22}n_{12} + m_{22}n_{21}] \\ 0.5[m_{12}n_{11} + m_{21}n_{11}] & 0.5[m_{12}n_{22} + m_{21}n_{22}] & 0.25[m_{12}n_{12} + m_{12}n_{21} + m_{21}n_{12} + m_{21}n_{21}] \end{bmatrix} \tag{212}$$

Henceforth, the dyadic product $\boldsymbol{s} \otimes \boldsymbol{s}$ in the case of von Mises plasticity with $\boldsymbol{m} = \boldsymbol{n} = \boldsymbol{s}$ reduces to the standard form,

$$\boldsymbol{s}_{voigt}\boldsymbol{s}^t_{voigt} = \begin{bmatrix} s_{11}s_{11} & s_{11}s_{22} & s_{11}s_{12} \\ s_{22}s_{11} & s_{22}s_{22} & s_{22}s_{12} \\ s_{12}s_{11} & s_{12}s_{22} & s_{12}s_{12} \end{bmatrix} \tag{213}$$

taking advantage of symmetry, when $s_{12} = s_{21}$.

## 8.2 Tensors

1. Stress and Strain Tensors: a set of objects $\boldsymbol{\sigma}, \boldsymbol{\epsilon} \in \Re^3$ which may be represented as $(3 \times 3)$ matrices whose coefficients are the coordinates of a set of orthonormal base vectors.

   (a) Scalar (inner) product of $\boldsymbol{\sigma}, \boldsymbol{\epsilon} \in \Re^3$: Double Contraction
   This product operation generates a scalar value:

   $$2W = \boldsymbol{\sigma} : \boldsymbol{\epsilon} = \sigma_{ij}\epsilon_{ij} \tag{214}$$

   Direction between two tensors:

   $$\cos\theta = \frac{\boldsymbol{\sigma} : \boldsymbol{\epsilon}}{\sigma\epsilon} \tag{215}$$

   where $0 \leq \theta \leq \pi/2$, and where $\sigma = (\boldsymbol{\sigma} : \boldsymbol{\sigma})^{\frac{1}{2}}$ and $\epsilon = (\boldsymbol{\epsilon} : \boldsymbol{\epsilon})^{\frac{1}{2}}$ are the Euclidean lengths of the two vectors.

Note: The internal strain energy is directly related to the scalar product of stress and strain.

(b) Outer product of $\boldsymbol{\sigma}, \boldsymbol{\epsilon} \in \Re^3$: Single Contraction This product operation generates a second order tensor:

$$2\boldsymbol{w} = \boldsymbol{\sigma} \cdot \boldsymbol{\epsilon} = \sigma_{ij}\epsilon_{jk} \tag{216}$$

Note: The thermodynamic force in the form of a tensor product of stress and strain is conjugate to the second order damage tensor.

(c) Dyadic or tensor product of $\boldsymbol{\sigma}, \boldsymbol{\epsilon} \in \Re^3$: No Contraction
This product operation generates a fourth order rank-one tensor:

$$2\boldsymbol{W} = \boldsymbol{\sigma} \otimes \boldsymbol{\epsilon} = \sigma_{ij}\epsilon_{kl} \tag{217}$$

Note: the tensorial order of the dyadic product is the sum the tensorial order of each factor. E.g. the dyadic product of two second order tensors generates a fourth order tensor, etc.

(d) Inverse of Rank-One Modification of Unit Tensor $\boldsymbol{I}$:

$$\boldsymbol{B} = \boldsymbol{I} + \boldsymbol{a} \otimes \boldsymbol{b} \quad \text{then} \quad \boldsymbol{B}^{-1} = \boldsymbol{I} - \frac{1}{1 + \boldsymbol{a} \cdot \boldsymbol{b}} \boldsymbol{a} \otimes \boldsymbol{b} \tag{218}$$

as long as $\boldsymbol{a} \cdot \boldsymbol{b} \neq -1$.

(e) Sherman-Morrison Formula of Inversion:

$$\boldsymbol{B} = \boldsymbol{A} + \boldsymbol{X} \otimes \boldsymbol{Y} \tag{219}$$

then

$$\boldsymbol{B}^{-1} = \boldsymbol{A}^{-1} - \frac{1}{1 + \boldsymbol{Y}\boldsymbol{A}^{-1}\boldsymbol{X}} \boldsymbol{A}^{-1}\boldsymbol{X} \otimes \boldsymbol{Y}\boldsymbol{A}^{-1} \tag{220}$$

(f) Outer products do not commute:

$$\boldsymbol{A} \cdot \boldsymbol{B} \neq \boldsymbol{B} \cdot \boldsymbol{A}, \quad \text{however} \quad \boldsymbol{B} \cdot \boldsymbol{A} = [\boldsymbol{A}^t \cdot \boldsymbol{B}^t]^t \tag{221}$$

This also holds for tensor products.

## 8.3 Determinant:

The determinant of a second order tensor is a single number which summarizes the tensorial property in the form of a multi-linear functional.

i. Determinant of tensor products:

$$\det(\boldsymbol{A} \cdot \boldsymbol{B}) = \det \boldsymbol{A} \det \boldsymbol{B} \tag{222}$$

ii. The Schur theorem states that the determinant of partitions in tensor $\boldsymbol{A}$ may be written in terms of the determinant product of partitions:

$$\det \boldsymbol{A} = \det \boldsymbol{A}_{22} \det \boldsymbol{A}_{11}^{compl} = \det \boldsymbol{A}_{22} \det(\boldsymbol{A}_{11} - \boldsymbol{A}_{12}\boldsymbol{A}_{22}^{-1}\boldsymbol{A}_{21}) \tag{223}$$

Note: The Schur complement couples the partitions and leads to the bound $\det \boldsymbol{A} \leq \det \boldsymbol{A}_{22} \det \boldsymbol{A}_{11}$ as long as $\boldsymbol{x} \cdot \boldsymbol{A}_{22} \cdot \boldsymbol{x} > 0$ is positive definite.

## 8.4 Eigenvalues and Eigenvectors:

There exist a nonzero vector $\boldsymbol{x}$ such that the linear transformation $\boldsymbol{\sigma} \cdot \boldsymbol{x}$ is a multiple of $\boldsymbol{x}$

$$\boldsymbol{\sigma} \cdot \boldsymbol{x} = \lambda \boldsymbol{x} \tag{224}$$

Note: The eigenvector $\boldsymbol{x}_i$ spans the triad of principal directions and the eigenvalues $\lambda_i$ define the three principal values of stress.

i. Characteristic Polynomial:
The eigenvalue problem is equivalent to stating that

$$(\boldsymbol{\sigma} - \lambda \boldsymbol{I}) \cdot \boldsymbol{x} = \boldsymbol{0} \tag{225}$$

For a non-trivial solution $\boldsymbol{x} \neq \boldsymbol{0}$ then $(\boldsymbol{\sigma} - \lambda_i \boldsymbol{I})$ must be singular. Consequently,

$$\det(\boldsymbol{\sigma} - \lambda \boldsymbol{I}) = 0 \tag{226}$$

generates the characteristic polynomial

$$p(\lambda) = \det(\boldsymbol{\sigma} - \lambda \boldsymbol{I}) \tag{227}$$

the roots of which are the eigenvalues $\lambda(\boldsymbol{\sigma})$. According to the fundamental theorem of algebra, a polynomial of degree 3 has exactly 3 roots, thus each matrix $\boldsymbol{\sigma} \in \Re^3$ has 3 eigenvalues.
Note: all three eigenvalues are real as long as $\boldsymbol{\sigma} = \boldsymbol{\sigma}^t$ is symmetric which is the case for non-polar materials because of conjugate shear stresses $\sigma_{ij} = \sigma_{ji}$.

ii. Cayley-Hamilton Theorem:
This theorem states that every square matrix satisfies its own characteristic equation. In other terms the scalar polynomial $p(\lambda) = \det(\lambda \boldsymbol{I} - \boldsymbol{\sigma})$ also holds for the stress polynomial $p(\boldsymbol{\sigma})$. One important application of the Cayley-Hamilton theorem is to express powers of the stress tensor $\boldsymbol{\sigma}^k$ as linear combination of the irreducible bases $\boldsymbol{I}, \boldsymbol{\sigma}, \boldsymbol{\sigma}^2$ for $k \geq 2$.

iii. Spectral Properties of Rank-One Update of Unit Tensor:
Spectral analysis of square matrix generated by a rank-one update of the unit tensor of second order

$$\boldsymbol{B} = \boldsymbol{I} + \boldsymbol{a} \otimes \boldsymbol{b} \tag{228}$$

reduces to the eigenvalue analysis

$$[(\boldsymbol{b}\cdot\boldsymbol{a}-(\lambda-1)]\,\boldsymbol{a}=\boldsymbol{0} \tag{229}$$

The eigenvalues and eigenvectors of $\boldsymbol{B}=\boldsymbol{I}+\boldsymbol{a}\otimes\boldsymbol{b}$ are related to the eigenpairs of the update matrix, i.e.

$$\lambda(\boldsymbol{B})=1+\lambda \quad \text{and} \quad \boldsymbol{x}(\boldsymbol{B})=\boldsymbol{a} \tag{230}$$

In the case of a single rank-one update of the unit matrix we find $\lambda_1(\boldsymbol{B})=1+\lambda$ and $\lambda_k(\boldsymbol{B})=1\forall k=2,3..n$ with the determinant $\det(\boldsymbol{B})=\det(\boldsymbol{I}+\boldsymbol{a}\otimes\boldsymbol{b})=1+\boldsymbol{a}\cdot\boldsymbol{b}$, and $\lambda=\boldsymbol{a}\cdot\boldsymbol{b}$.

# 9 Appendix II: Plane Strain Constraint of Elastoplastic Limit Point

On a final note, we observe that the kinematic constraint of zero out-of-plane deformations delays and may suppress altogether the formation of a limit point associated with peak strength in pressure-sensitive plasticity. We recall the shear response does not reach a limit point under plane strain. The reason for this puzzling observation is the kinematic constraint which restricts the formation of a limit point when

$$\dot{\boldsymbol{\sigma}}=\boldsymbol{\mathcal{E}}:[\dot{\boldsymbol{\epsilon}}-\dot{\boldsymbol{\epsilon}}_p]=\boldsymbol{0} \quad \text{where} \quad \dot{\boldsymbol{\epsilon}}_p=\dot{\lambda}\boldsymbol{m} \tag{231}$$

In the plastic flow rule $\dot{\lambda}$ denotes the plastic multiplier, which is strictly positive under sustained plastic flow, and $\boldsymbol{m}=\frac{\partial Q}{\partial\boldsymbol{\sigma}}$ the direction of plastic flow in terms of the gradient of the plastic potential. Consequently, the only possibility to form a limit point at peak occurs if the strain rate equals the plastic strain rate, $\dot{\boldsymbol{\epsilon}}=\dot{\boldsymbol{\epsilon}}_p$ and the elastic strain rate remains zero, $\dot{\boldsymbol{\epsilon}}_e=\boldsymbol{0}$.

The plane strain constraint infers that the out-of-plane strain rate must vanish, i.e.

$$\dot{\epsilon}_{33}=\dot{\lambda}m_{33}=\dot{\lambda}\frac{\partial Q}{\partial\sigma_{33}}=0 \tag{232}$$

In the three-invariant plasticity formulation above this constraint implies that

$$m_{33}=\frac{1}{\sqrt{3}}(Q_\xi-\frac{Q_\theta}{\tau_{12}})=0 \quad \text{or} \quad Q_\xi=\frac{Q_\theta}{\tau_{12}} \tag{233}$$

In short, pressure sensitive plastic flow, $Q_\xi\neq 0$, does not permit formation of a limit point as shown in Figures 8 and 13. And even if this would be the case, the shear stress would never reach the peak value because loss of stability and localization take place much earlier in the ascending regime of apparent hardening.